

References

1. M. Ramalho-Santos, and H. Willenbring, On the origin of the term "stem cell", *Cell Stem Cell.*, 1, 35-38, 2007.
2. R. Prakash, S. K. Yadav, and S. S. Raza, Stem cells therapy in human welfare and disease, *Era's j. med. res.*, 7, 1-6, 2020.
3. W. Zakrzewski, M. Dobrzyński, M. Szymonowicz, et al., Stem cells: past, present, and future, *Stem Cell Res Ther.*, 10, 68, 2019.
4. J. A. Thomson, J. Itskovitz-Eldor, S. S. Shapiro, M. A. Waknitz, J. J. Swiergiel, et. al., Embryonic Stem Cell Lines Derived from Human Blastocysts, *Science*, 282, 1145-1147, 1998.
5. M. T. Little, and R. Storb, History of haematopoietic stem-cell transplantation. *Nat Rev Cancer* 2, 231–238.
6. C. Eguizabal, B. Aran, S. M. C. de Sousa Lopes, M. Geens, B. Heindryckx, S. Panula, et. al., Two decades of embryonic stem cells: a historical overview, *Human Reproduction Open*, 2019;1, hoy024, 2019.
7. U. Lendahl, L. B. Zimmerman, R. and D. G. McKay, CNS stem cells express a new class of intermediate filament protein, *Cell*, 23, 585-595, 1990.
8. E. Ratcliffe, K. E. Glen, M. W. Naing, and D. J. Williams, Current status and perspectives on stem cell-based therapies undergoing clinical trials for regenerative medicine: case studies, *Br Med Bull.*, 108, 73-94, 2013.
9. E. Jacques, and E. J. Suuronen, The Progression of Regenerative Medicine and its Impact on Therapy Translation, *Clin Transl Sci.* 13;3, 440-450, 2020.
10. A. Chhabra, Derivation of Human Induced Pluripotent Stem Cell (iPSC) Lines and Mechanism of Pluripotency: Historical Perspective and Recent Advances, *Stem Cell Rev and Rep.*, 13, 757–773, 2017.
11. M. Liu, J. Tu, J.A. Gingold, C. S. L. Kong, and D. F. Lee, Cancer in a dish: progress using stem cells as a platform for cancer research, *Am J Cancer Res.*, 1;8, 944-954, 2018.
12. Y. Shen, Stem cell therapies for retinal diseases: from bench to bedside, *J Mol Med.*, 98, 1347–1368, 2020.
13. D. De, P. Karmakar, and D. Bhattacharya, Stem Cell Aging and Regenerative Medicine. *Adv. Exp. Med. Biol.A.*, 12, 1326, 2020.
14. G. Liu, B. T. David, M. Trawczynski, and R. G. Fessler, Advances in Pluripotent Stem Cells: History, Mechanisms, Technologies, and Applications, *Stem Cell Rev.*, 16,1, 3-32, 2020.
15. L. L. N. M. Lopes, T. P. Navarro, and A. Dardik, Introduction to Stem Cell Therapy and Its Application in Vascular Diseases, *Springer Cham.*, 1-32, 2021.
16. F. F. Rosa, C. F. Pires, I. Kurochkin, A. G. Ferreira, A. M. Gomes, et al., Direct reprogramming of fibroblasts into antigen-presenting dendritic cells, *Sci Immunol.*, 3, 30, eaau4292, 2018.
17. R. K. Gupta, D. Peppas, A. L. Hill, C. Galvez, and M. Salgado, Evidence for HIV-1 cure after *CCR5*Δ32/Δ32 allogeneic haematopoietic stem-cell transplantation 30 months post analytical treatment interruption: a case report, *Lancet HIV*, 5, e340-e347, 2020.
18. I. A. Charitos, A. Ballini, S. Cantore, M. Boccellino, M. Di Domenico, et al., Stem Cells: A Historical Review about Biological, Religious, and Ethical Issues, *Stem Cells Int.*, 29, 2021.

19. M. S. Elitt, L. Barbar, and P. J. Tesar, Drug screening for human genetic diseases using iPSC models, *Hum. Mol. Genet.*, 27, R89–R98, 2018.
20. O. Z. Fisher, A. Khademhosseini, R. Langer, and N. A. Peppas, Bioinspired materials for controlling stem cell fate, *Acc Chem Res.*, 43,3, 419-28, 2010.
21. J. K. Yoon, M. L. Kang, J. H. Park, K. M. Lee, Y. M. Shin, et al., Direct Control of Stem Cell Behavior Using Biomaterials and Genetic Factors, *Stem Cells Int.*, 8642989, 2018.
22. L. Latxague, M. A. Ramin, A. Appavoo, P. Berto, M. Maisani, et al., Control of stem-cell behavior by fine tuning the supramolecular assemblies of low-molecular-weight gelators, *Angew Chemie Int. Ed. Engl.*, 54;15, 4517-4521, 2015.
23. J. S. Choi, and B. A. Harley, Challenges and Opportunities to Harnessing the (Hematopoietic) Stem Cell Niche, *Curr Stem Cell Rep.*, 2;1, 85-94, 2016.
24. Q. Sun, Z. Zhang, and Z. Sun, The potential and challenges of using stem cells for cardiovascular repair and regeneration, *Genes Dis.*, 1;1, 113-119, 2014.
25. P. X. Wan, B. W. Wang, and Z. C. Wang, Importance of the stem cell microenvironment for ophthalmological cell-based therapy, *World J Stem Cells*, 7;2, 448-460, 2015.
26. D. T. Scadden, The stem-cell niche as an entity of action, *Nature*, 441; 7097, 1075–92, 2006.
27. R. O. Hynes, The extracellular matrix: not just pretty fibrils, *Science*, 326, 1216–1219, 2009.
28. A. Page-McCaw, A. J. Ewald, and Z. Werb, Matrix metalloproteinases and the regulation of tissue remodelling, *Nat Rev Mol Cell Biol.*, 8, 221–233, 2007.
29. S. Ozbek, P. G. Balasubramanian, R. Chiquet-Ehrismann, R. P. Tucker, and J. C. Adams, The evolution of extracellular matrix, *Mol Biol Cell.*, 21, 4300–43002, 2010.
30. P. Lu, V. M. Weaver, and Z. Werb, The extracellular matrix: a dynamic niche in cancer progression, *J Cell Biol.*, 196, 395–406, 2012.
31. V. Marx, Where stem cells call home, *Nat Methods*, 10,2, 111-115, 2013.
32. R. Peerani, and P. W. Zandstra, Enabling stem cell therapies through synthetic stem cell-niche engineering, *J Clin Invest*, 120, 60-70, 2010.
33. M. C. Prewitz, F. P. Seib, M. V. Bonin, J. Friedrichs, A. Stiel, et al., Tightly anchored tissue- mimetic matrices as instructive stem cell microenvironment, *Nat Methods*, 10;8, 788-794, 2013.
34. P. Wu, D. G. Castner, and D. W. J. Grainger, Diagnostic devices as biomaterials: a review of nuclei acid and protein microarray surface performance issues, *J Biomater Sci Polym Ed*, 19, 725-753, 2008.
35. K. Ghosh, and D. E. Ingber, Micromechanical control of cell and tissue development: Implications for tissue engineering, *Adv Drug Deliv Rev.*, 59, 1306-1318, 2007.
36. K. A. Kilian, B. Bugarija, B. T. Lahn, and Mrksich, Geometric cues for directing the differentiation of mesenchymal stem cells, *Proc Nat l Acad Sci USA*, 107, 4872-4877, 2010.
37. K. Kolind, K. W. Leong, F. Besenbacher, and M. Foss, Guidance of stem cell fate on 2D patterned surfaces, *Biomater.*, 33, 6626-6633, 2012.
38. A. M. Ross, Z. Jiang, M. Bastmeyer, and J. Lahann, Physical aspects of cell culture substrates: topography, roughness, and elasticity, *Small*, 8; 3, 336-355, 2012.
39. A. Bédier, C. Vieu, F. Arnauduc, J. C. Sol, I. Loubinoux, and L. Vaysse, Engineering of adult human neural stem cells differentiation through surface micropatterning, *Biomater.*, 33, 504-514, 2012.

40. D. Khang, J. Choi, Y. M. Im, Y. J. Kim, J. H. Jang, et al., Role of subnano-, nano-, and submicron-surface features on osteoblast differentiation of bone marrow mesenchymal stem cells, *Biomater.*, 33;26, 5997-6007, 2012.
41. G. Kumar, C. K. Tison, K. Chatterjee, P. S. Pine, J. H. McDaniel, et al., The determination of stem cell fate by 3D scaffold structures through the control of cell shape, *Biomater.*, 32, 9188-9196, 2011.
42. A. J. Engler, S. Sen, H. L. Sweeney, and D. E. Discher, Matrix elasticity directs stem cell lineage specification, *Cell.*, 126, 677-689, 2006.
43. D. S. W. Benoit, M. P. Schwartz, A. R. Durney, and K. S. Anseth, Small functional groups for controlled differentiation of hydrogel-encapsulated human mesenchymal stem cells, *Nat. Mat.*, 7, 816- 823, 2008.
44. E. K. F. Yim, E. M. Darling, K. Kulangara, F. Guilak, and K. W. Leong, Nanotopography-induced changes in focal adhesions, cytoskeletal organization, and mechanical properties of human mesenchymal stem cells, *Biomater.*, 31, 1299, 2010.
45. P. M. Gilbert, K. L. Havenstrite, K. E. Magnusson, A. Sacco, N. A. Leonardi, et al., Substrate elasticity regulates skeletal muscle stem cell self-renewal in culture, *Science*, 27, 1078-81, 2010.
46. R. A. Marklein, and J. A. Burdick, Controlling Stem Cell Fate with Material Design, *Adv. Mater.*, 22, 175-189, 2010.
47. X. Hu, S. H. Park, E. S. Gil, X. X. Xia, A. S. Weiss, et. al., The influence of elasticity and surface roughness on myogenic and osteogenic-differentiation of cells on silk-elastin biomaterials, *Biomater.*, 32, 8979-8989, 2011.
48. A. Solanki, S. T. Chueng, P. T. Yin, R. Kappera, M. Chhowalla, et al., Axonal Alignment and Enhanced Neuronal Differentiation of Neural Stem Cells on Graphene-Nanoparticle Hybrid Structures, *Adv. Mater.*, 25;38, 5477-82, 2013.
49. M. Tang, Q. Song, N. Li, Z. Jiang, R. Huang, et al., Enhancement of electrical signaling in neural networks on graphene films, *Biomater.*, 34, 6402-6411, 2013.
50. K. H. Park, and M. Dhayal, 3D-nanoflowers of rutile TiO₂ as a film grown on conducting and non-conducting glass substrates for in vitro biocompatibility studies with mouse MC3T3 osteoblast and human HS-5 cells, *RSC Adv.*, 5, 33503-33514, 2015.
51. J. Leijten, and A. Khademhosseini, From Nano to Macro: Multiscale Materials for Improved Stem Cell Culturing and Analysis. *Cell Stem Cell.*, 18, 20-24, 2016.
52. X. Lin, Y. Shi, Y. Cao, and W. Liu, Recent progress in stem cell differentiation directed by material and mechanical cues, *Biomed. Mater.*, 11, 014109, 2016.
53. D. A. Balikov, B. Fang, Y.W. Chun, S. W. Crowder, D. Prasai, et al., Directing lineage specification of human mesenchymal stem cells by decoupling electrical stimulation and physical patterning on unmodified graphene, *Nanoscale*, 8, 13730-13739, 2016.
54. M. Wei, S. Li, and W. Le, Nanomaterials modulate stem cell differentiation: biological interaction and underlying mechanisms, *J Nanobiotechnol.*, 15, 1-13, 2017.
55. M. J. Gupte, W. B. Swanson, J. Hu, X. Jin, H. Ma, et al., Pore size directs bone marrow stromal cell fate and tissue regeneration in nanofibrous macroporous scaffolds by mediating vascularization, *Acta biomater.*, 82, 1-11, 2018.
56. C. M. Madl, and S. C. Heilshorn, Engineering hydrogel microenvironments to recapitulate the stem cell niche, *Annu. Rev. Biomed. Eng.*, 20, 21-47, 2018.
57. M. Chen, Y. Hu, M. Li, M. Chen, X. Shen, et al., Regulation of osteoblast differentiation by osteocytes cultured on sclerostin antibody conjugated TiO₂ nanotube array, *Colloids Surf B Biointerfaces.*, 175, 663-670, 2019.

58. M. Farokhi, F. Mottaghitlab, M. R. Saeb, Shahrokh Shojaei, N. K. Zarrin, et al., Conductive Biomaterials as Substrates for Neural Stem Cells Differentiation towards Neuronal Lineage Cells, *Macromol Biosci.*, 21;1, 2000123, 2020.
59. J. Du, C. Agatemor, C. T. Saeui, R. Bhattacharya, X. Jia, et al., Glycoengineering Human Neural and Adipose Stem Cells with Novel Thiol-Modified N-Acetylmannosamine (ManNAc) Analogs, *Cells.*, 10, 377, 2021.
60. Y. W. Cho, S. Jee, I. R. Suhito, J. H. Lee, C. G. Park, et al., Single metal-organic framework-embedded nanopit arrays: A new way to control neural stem cell differentiation, *Sci. Adv.*, 8,16, eabj7736, 2022.
61. B. Westermann, Mitochondrial fusion and fission in cell life and death, *Nat. Rev. Mol. Cell Biol.*, 11, 872–884, 2010.
62. T. Simsek, F. Kocabas, J. Zheng, R. J. Deberardinis, A. I. Mahmoud, et al., The distinct metabolic profile of hematopoietic stem cells reflects their location in a hypoxic niche, *Cell Stem Cell.*, 7, 380–390, 2010.
63. T. Suda, K. Takubo, and G. L. Semenza, Metabolic regulation of hematopoietic stem cells in the hypoxic niche, *Cell Stem Cell.*, 9, 298–310, 2011.
64. S. Papa, P. L. Martino, G. Capitanio, A. Gaballo, D. de Rasmio, et al., The oxidative phosphorylation system in mammalian mitochondria, *Adv. Exp. Med. Biol.*, 942, 3–37, 2012.
65. F. M. Tonelli, A. K. Santos, D. A. Gomes, S. L. da Silva, K. N. Gomes, et al., Stem cells and calcium signaling, *Adv Exp Med Biol.*, 740, 891-916, 2012.
66. O. Forostyak, N. Romanyuk, A. Verkhatsky, E. Sykova, and G. Dayanithi, Plasticity of calcium signaling cascades in human embryonic stem cell-derived neural precursors, *Stem Cells Dev.*, 22; 10, 1506–1521, 2013.
67. G. G. Nair, J. S. Liu, H. A. Russ, S. Tran, M. S. Saxton, et al., Recapitulating endocrine cell clustering in culture promotes maturation of human stem-cell-derived β cells, *Nat Cell Biol.*, 21, 263–274, 2019.
68. C. N. R. Rao, and A. K. Cheetham, Science and technology of nanomaterials: current status and future prospects, *J. Mater. Chem.*, 11, 2887-2894, 2001.
69. H. S. Nalwa, Encyclopedia of nanoscience and nanotechnology, American Scientific Publisher: USA, 2011.
70. S. T. Aruna, and A. S. Mukasyan, Combustion synthesis and nanomaterials, *Curr. Opin. Solid State Mater. Sci.*, 12, 44-50, 2008.
71. P. Yang, D. Zhao, D. I. Margolese, B. F. Chmelka, and G. D. Stucky, Generalized syntheses of large-pore mesoporous metal oxides with semicrystalline frameworks, *Nature*, 396, 152-155, 1998.
72. J. Li, S. Tang, L. Lu, and H. C. Zeng, Preparation of Nanocomposites of Metals, Metal Oxides, and Carbon Nanotubes via Self-Assembly, *J. Am. Chem. Soc.*, 129, 9401-9409, 2007.
73. B.D. Ratner and S.J. Bryant, Biomaterials: where we have been and where we are going, *Annu. Rev. Biomed. Eng.*, 6, 41-75, 2004.
74. C. Loty, J.M. Sautier, M.T. Tan, M. Oboeuf, E. Jallot, et al., Bioactive Glass Stimulates In Vitro Osteoblast Differentiation and Creates a Favorable Template for Bone Tissue Formation, *J. Bone Miner. Res.*, 16: 231–239, 2001.
75. S. Mandl, Increased Biocompatibility and Bioactivity after Energetic PVD Surface Treatments, *Materials.*; 2, 1341-1387, 2009.

76. R. F. Brow, D. E. Day, T. E. Day, S. Jung, M. N. Rahaman, et al., Growth and differentiation of osteoblastic cells on 13–93 bioactive glass fibers and scaffolds, *Acta Biomater.*, 4, 387-396, 2008.
77. M. Dhayal, R. Kapoor, P. G. Sistla, C. Kant, R. R. Pandey, et. al., Ni doped TiO₂ thin films on borosilicate glass enhance in-vitro growth and differentiation of osteoblasts, *J. Biomed. Mat. Res. Part A.*, 100A, 1168-1178, 2012.
78. W. Zhao, C. Chen, W. Ma, J. Zhao, and Z Shuai, Efficient degradation of toxic organic pollutants with Ni₂O₃/TiO_{2-x}B_x under visible irradiation, *J. Am. Chem. Soc.*, 126, 4782-4783, 2004.
79. A. J. Maira, K. L. Yeung, C. Y. Lee, P. L. Yue, and C. K. Chan, Size effects in gas-phase photo-oxidation of trichloroethylene using nanometer-sized TiO₂ catalysts, *J. Catal.*, 192, 185-196, 2000.
80. R. Carbone, I. Marangi, A. Zanardi, L. A Giorgetti, E. Chierici, et.al., Biocompatibility of cluster-assembled nanostructured TiO₂ with primary and cancer cells. *Biomaterials*, 27, 3221-3229, 2006.
81. M. Dhayal, R. Kapoor, P. G. Sistla, R. R. Pandey, S. Kar, et. al., Strategies to prepare TiO₂ thin films, doped with transition metal ions, that exhibit specific physicochemical properties to support osteoblast cell adhesion and proliferation. *Mat. Sci.Eng. C.*, 37, 99–107, 2014.
82. S. Rossi, N. Moritz, T. Tirri, T. Peltola, S. Areva, et. al., Comparison between sol-gel-derived anatase- and rutile-structured TiO₂ coatings in soft-tissue environment, *J. Biomed. Mater. Res.*, 82, 965–974, 2007.
83. W. Han, Y. Wang, and Y. Zheng, In vivo biocompatibility studies of nano TiO₂ materials. *Adv. Mat. Res.*, 79, 389-392, 2009.
84. R. Karpagavalli, A. Zhou, P. Chellamuthu, and K. Nguyen, Corrosion behavior and biocompatibility of nanostructured TiO₂ film on Ti6Al4V, *J. Biomed. Mater. Res. A.*, 83, 1087-1095, 2007.
85. K. Anselme, Osteoblast adhesion on biomaterials, *Biomaterials*, 21(7): 667-681,2000.
86. S. Foppiano, S.J. Marshall, G.W. Marshall, E. Saiz, and A.P. Tomsia, The influence of novel bioactive glasses on in vitro osteoblast behavior, *J. Biomed. Mater. Res.*, 71A, 242–249, 2004.
87. M. Dhayal, S. I. Cho, J. Y. Moon, S. J. Cho, and A. Zykova, S180 cell growth on low ion energy plasma treated TiO₂ thin films, *Appl. Surf. Sci.*, 254, 3331-3338, 2008.
88. K. H. Park, and M. Dhayal, Simultaneous growth of rutile TiO₂ as 1D/3Dnanorod/nanoflower on FTO in one-step process enhances electrochemical response of photoanode in DSSC, *Electrochem. Commun.*, 49, 47-50, 2014.
89. H. Zhang, Y. Han, X. Liu, P. Liu, Yu H., et al., Anatase TiO₂ microspheres with exposed mirror-like plane {001} facets for high performance dye-sensitized solar cells (DSSCs), *Chem. Comm.*, 46, 8395-8397, 2010.
90. Y. Li, Q. Sun, X. Sun, and L. Dong, Synthesis of nanocoral structured TiO₂ and its photoelectrical performance in dye sensitized solar cells, *ECS. Trans.*, 53, 57-63, 2013.
91. L. L. Li, Y. J. Chen, H. P. Wu, N. S. Wang, and E.W.G. Diau, Detachment and transfer of ordered TiO₂ nanotube arrays for front-illuminated dye-sensitized solar cells. *Energ. Environ. Sci.*, 4, 3420-3425, 2011.
92. J. Qu, and C. Lai, One-dimensional nanostructures as photoanodes for dye-sensitized solar cells, *J. Nanomater.*, 762730, 2013.
93. M. Adachi, Y. Murata, J. Takao, J. Jiu, M. Sakamoto, et. al., Highly efficient dye-sensitized solar cells with a titania thin-film electrode composed of a network structure

- of single-crystal-like TiO₂ nanowires made by the “oriented attachment” mechanism, *J. Am. Chem. Soc.*, 126, 14943-14949, 2004.
94. K. N. Pandiyaraj, V. Selvarajan, M. Pavese, P. Falaras, and D. Tsoukleris, Investigation on surface properties of TiO₂ films modified by DC glow discharge Plasma, *Curr. Appl. Phys.*, 9, 1032-1037, 2009.
 95. I. Ichinose, H. Senzu, and T. Kunitake, Stepwise adsorption of metal alkoxides on hydrolyzed surfaces: A surface sol–gel process, *Chem. Lett.*, 25, 831-832, 1996.
 96. B. D. Boyan, T. W. Hummert, D. D. Dean, and Z. Schwartz, Role of material surfaces in regulating bone and cartilage cell response, *Biomater.*, 17, 137-146, 1996.
 97. K. H. Park, and M. Dhayal, 3D-nanoflowers of rutile TiO₂ as a film grown on conducting and non-conducting glass substrates for in vitro biocompatibility studies with mouse MC3T3 osteoblast and human HS-5 cells, *RSC Adv.*, 5, 33503-33514, 2015.
 98. S. Q. Liu, *Bioregenerative Engineering: Principles and Applications*, Wiley-Intersci. Publ., 2007.
 99. P.X. Ma, Biomimetic materials for tissue engineering, *Adv. Drug. Deliv. Rev.*, 60, 184-198, 2008.
 100. X. Liu, and C. Ding, Plasma sprayed wollastonite/TiO₂ composite coatings on titanium alloys, *Biomaterials*, 23, 4065-4077, 2002.
 101. D.S. Kommireddy, S.M. Sriram, Y.M. Lvov, and D.K. Mill, Stem cell attachment to layer-by-layer assembled TiO₂ nanoparticle thin films, *Biomaterials*, 27, 4296-4303, 2006.
 102. D.R. Uhlmann, T. Suratwala, K. Davidson, J.M. Boulton, and G. Teowee, Sol-gel derived coatings on glass, *J. Non-Cryst. Solids*, 218, 113-122, 1997.
 103. A. Tricoli, M. Righettoni, and S.E. Pratsinis, Anti-Fogging Nanofibrous SiO₂ and Nanostructured SiO₂-TiO₂ Films Made by Rapid Flame Deposition and In Situ Annealing, *Langmuir*, 21, 12578–12584, 2009.
 104. M. Dhayal, S.D. Sharma, C. Kant, K.K. Saini, and S.C. Jain, Role of Ni doping in surface carbon removal and photo catalytic activity of nano-structured TiO₂ film, *Surf. Sci.*, 602, 1149- 1154, 2008.
 105. X.Y. Jing, and S. D. Chen, *Guide of Infrared Spectroscopy*, Tianjin: Tianjin Science and Technology Press, 1–120, 1992.
 106. C. S. Kuo, Y. H. Tseng, C. H. Huang and Y. Y. Li, Carbon-containing nanotitania prepared by chemical vapor deposition and its visible-light-responsive photocatalytic activity, *J. Mol. Catal.*, 270, 93–100, 2007.
 107. Y. Cheng, H. Sun, W. Jin, and N. Xu, Photocatalytic degradation of 4-chlorophenol with combustion synthesized TiO₂ under visible light irradiation, *Chem. Eng. J.*, 128, 127–133, 2007.
 108. J. Qu, and C. Lai One-Dimensional Nanostructures as Photoanodes for Dye-Sensitized Solar Cells. *J. Nanomater.*, 762730, 2013.
 109. P.X. Ma, Biomimetic materials for tissue engineering, *Adv. Drug. Deliv. Rev.*, 60, 184-198, 2008.
 110. T. Mazza, E. Barborini, P. Piseri, P. Milani, D. Cattaneo, et al., Raman spectroscopy characterization of TiO₂ rutile nanocrystals. *Phys. Rev. B*, 75, 4-15, 2007.
 111. M. Adachi, Y. Murata, J. Takao, Jiu J.; Sakamoto M.; Wang F. Highly Efficient Dye-Sensitized Solar Cells with a Titania Thin-Film Electrode Composed of a Network Structure of Single-Crystal-like TiO₂ Nanowires Made by the “Oriented Attachment” Mechanism, *J. Am. Chem. Soc.*, 126, 14943-14949, 2004.

112. Y. Li, Q. Sun, X. Sun, and L. Dong, Synthesis of Nanocoral Structured TiO₂ and its Photoelectrical Performance in Dye Sensitized Solar Cells, *ECS Trans.*, 53, 57-63, 2013.
113. H. Zhang, Y. Han, X. Liu, P. Liu, H. Yu, et. al., Anatase TiO₂ microspheres with exposed mirror-like plane {001} facets for high performance dye-sensitized solar cells (DSSCs), *Chem. Comm.*, 46, 8395-8397, 2010.
114. L. L. Li, Y. J. Chen, H. P. Wu, N. S. Wang, and E.W.G. Diau, Detachment and transfer of ordered TiO₂ nanotube arrays for front-illuminated dye-sensitized solar cells, *Energ. Environ. Sci.*, 4, 3420-3425, 2011.
115. A. Yella, H. W. Lee, H. N. Tsao, C. Y. Yeh, A. K. Chandira, et al., Porphyrin-Sensitized Solar Cells with Cobalt (II/III)-Based Redox Electrolyte Exceed 12 Percent Efficiency, *Science*, 334, 629-634, 2011.
116. Z. Sun, J. H. Kim, Y. Zhao, D. Attard, and S. X. Dou, Morphology-controllable 1D-3D nanostructured TiO₂ bilayer photoanodes for dye-sensitized solar cells, *Chem. Comm.*, 49, 966-968, 2013.
117. T. Mazza, E. Barborini, P. Piseri, P. Milani, D. Cattaneo, et al., Raman spectroscopy characterization of TiO₂ rutile nanocrystals. *Phys. Rev. B*, 75, 4-15, 2007.
118. M. Dhayal, S. I., Cho, J. Y. Moon, S. J. Cho, and A. Zykova, S180 cell growth on low ion energy plasma treated TiO₂ thin films, *Appl. Surf. Sci.*, 254, 3331-3338, 2008.
119. S. K. Vishwakarma, P. Sharmila, A. Bardia, L. Chandrakala, N. Raju, G. Sravani, B. V. S. Sastry, Md. A. Habeeb, A. K. Khan, M. Dhayal, Use of Biocompatible Sorafenib-gold Nanoconjugates for Reversal of Drug Resistance in Human Hepatoblastoma Cells, *Sci. Rep.*, 7, 8539, 2017.
120. S. K. Vishwakarma, J. Jaiswal, K. H. Park, C. Lakkireddy, N. Raju, et al., TiO₂ Nanoflowers on Conducting Substrates Ameliorate Effective Transdifferentiation of Human Hepatic Progenitor Cells for Long-Term Hyperglycemia Reversal in Diabetic Mice, *Adv. Therap.*, 3, 1900205, 2020.
121. M. E. Gindy, and R. K. Prudhomme, Multifunctional nanoparticles for imaging, delivery and targeting in cancer therapy, *Expert Opin. Drug Deliv.* 6, 865-878, 2009.
122. M. Niazi, P. Z. Milani, S. N. Hajivar, M. S. Goloujeh, N. Ghobakhlou, et. al. Nano-based strategies to overcome p-glycoprotein-mediated drug resistance, *Expert Opin. Drug Metab. Toxicol.*, 12, 1021-1033, 2016.
123. X. D. Zhang, D. Wu, X. Shen, P. X. Liu, N. Yang, et. al. Size-dependent in vivo toxicity of PEG-coated gold nanoparticles, *Int. J. Nanomed.*, 6 2071-2081, 2011.
124. G. Vecchio, A. Galeone, V. Brunetti, G. Maiorano, L. Rizzello, et. al. Mutagenic effects of gold nanoparticles induce aberrant phenotypes in *Drosophila Melanogaster*, *Nanomed.*, 8, 1-7, 2012.
125. S. Fraga, H. Faria, M. E. Soares, J. A. Duarte, L. Soares, et. al. Influence of the surface coating on the cytotoxicity, genotoxicity and uptake of gold nanoparticles in human HepG2 cells, *J. Appl. Toxicol.*, 33, 1111-1119, 2013.
126. T. Zhonga, Z. Jianga, P. Wang, S. Biea, F. Zhang, et. al. Silk fibroin/copolymer composite hydrogels for the controlled and sustained release of hydrophobic/hydrophilic drugs, *Int. J. Pharm.*, 494, 264-270, 2015.
127. G. Yang, H. Lin, B. B. R, S. Yu, and R. S. Tuan, Multilayered polycaprolactone/gelatin fiber-hydrogel composite for tendon tissue engineering, *Acta Biomater.*, 35, 68-76, 2016.

128. R. A. Kyle, D. P. Steensma, and M. A. Shampo, Otto Wichterle-Inventor of the First Soft Contact Lenses, *Mayo Clin., Proc.* 91 45-46, 2016.
129. J. A. P. Dutra, S. G. Carvalho, A. C. D. Zampirolli, R. D. Daltoe, R. M. Teixeira, et. al. Papain wound dressings obtained from poly(vinyl alcohol)/calcium alginate blends as new pharmaceutical dosage form: Preparation and preliminary evaluation, *Eur. J. Pharm. Biopharm.* 113 (2017) 11–23.
130. N. A. Peppas, Y. Huang, M. T. Lugo, J. H. Ward, and J. Zhang, Physicochemical foundations and structural design of hydrogels in medicine and biology, *Annual Rev. Biomed. Eng.*, 2, 9-29, 2000.
131. N. Bhattarai, J. Gunn, and M. Zhang, Chitosan-based hydrogels for controlled, localized drug delivery, *Adv. Drug Deliv. Rev.*, 62, 83–99, 2010.
132. I. Sole, S. Vilchez, J. Miras, N. Montanya, M. J. García-Celma, et. al. DHA and L- carnitine loaded chitosan hydrogels as delivery systems for topical applications, *Colloids Surf. A: Physicochem. Eng. Asp.*, 525, 85–92, 2017.
133. N. Desai, Challenges in Development of Nanoparticle-Based Therapeutics, *AAPS J.*, 14, 282-295, 2012.
134. E. M. Hotze, T. Phenrat, and G. V. Lowry, Nanoparticle aggregation: challenges to understanding transport and reactivity in the environment, *J. Environ. Qual.*, 39, 1909- 1924, 2010.
135. G. Ceccone, and A. G. Shard, Preface: In Focus Issue on Nanoparticle Interfaces, *Biointerphases*, 11, 1-22016.
136. J. W. Ai, W. Liao, and Z. L. Ren, Enhanced anticancer effect of copper-loaded chitosan nanoparticles against osteosarcoma, *RSC Adv.*, 7 ,15971-15977, 2017.
137. V. Sorichetti, V. Hugouvieux, and W. Kob, Structure and Dynamics of a Polymer–Nanoparticle Composite: Effect of Nanoparticle Size and Volume Fraction, *Macromolecules*, 51, 5375–5391, 2018.
138. Y. Zare, I. Shabani, Polymer/metal nanocomposites for biomedical applications, *Mater. Sci. Eng. C*, 60, 195-203, 2016.
139. H. Huang, X. Yang, Synthesis of Chitosan-Stabilized Gold Nanoparticles in the Absence/Presence of Tripolyphosphate, *Biomacromolecules*, 5, 2340-2346, 2004.
140. H. Huang, Q. Yuanb, X. Yang, Morphology study of gold–chitosan nanocomposites, *J. Colloid and Interface Sci.*, 282, 26–31, 2005.
141. M. M. Mohamed, S. A. Fouad, H. A. Elshoky, G. M. Mohammed, T. A. Salaheldin, Antibacterial effect of gold nanoparticles against *Corynebacterium pseudotuberculosis*, *Int. J. Vet.*, 5, 23-29, 2017.
142. R. L. Narayanan, M. Sivakumar, Preparation and Characterization of Gold Nanoparticles in Chitosan Suspension by one-pot Chemical Reduction Method, *Nano Hybrids*, 6, 47-57, 2014.
143. R. P. Ramasamy, S. M. Maliyekkal, Formation of gold nanoparticles upon chitosan leading to formation and collapse of gels, *New J. Chem.*, 38, 63-69, 2014.
144. K. D. N. Vo, E. Guillon, L. Dupont, C. Kowandy, X. Coqueret, Influence of Au(III) Interactions with Chitosan on Gold Nanoparticle Formation, *J. Phys. Chem. C*, 118, 4465-4474, 2014.
145. A. Sugunana, C. Thanachayanont, J. Dutta, J. G. Hilborn, Heavy-metal ion sensors using chitosan-capped gold nanoparticles, *Sci. Technol. Adv. Mater.*, 6, 335-340, 2005.

146. D. Wei, Y. Ye, X. Jia, C. Yuan, W. Qian, Chitosan as an active support for assembly of metal nanoparticles and application of the resultant bioconjugates in catalysis, *Carbohydr. Res.*, 345, 74-81, 2010.
147. W. B. Tan, Y. Zhang, Surface modification of gold and quantum dot nanoparticles with chitosan for bioapplications, *J. Biomed. Mater. Res. A.*, 75, 56-62, 2005.
148. E. Guibal, T. Vincent, R. Navarro, Metal ion biosorption on chitosan for the synthesis of advanced materials, *J. Mater. Sci.*, 49, 5505-5518, 2014.
149. N. C. Braier, R. A. Jishi, Density functional studies of Cu²⁺ and Ni²⁺ binding to chitosan. *J. Mol. Struct.*, 499, 51-55, 2000.
150. Y. Wu, F. Zuo, Y. Lin, Y. Zhou, Z. Zheng, X. Ding, Green and Facile Synthesis of Gold Nanoparticles Stabilized by Chitosan, *Journal of Macromolecular Science, Part A: Pure Appl. Chem.* 51, 441-446, 2014.
151. L. Jin, R. Bai, Mechanisms of Lead Adsorption on Chitosan/PVA Hydrogel Beads, *Langmuir*, 18, 9765-9770, 2002.
152. A. Pestova, A. Nazirovb, E. Modinc, A. Mironenkob, S. Bratskayab, Mechanism of Au(III) reduction by chitosan: Comprehensive study with ¹³C and ¹H NMR analysis of chitosan degradation products, *Carbohydr. Polym.*, 117, 70-77, 2015.
153. S. V. Agrawal, S. S. Reddy, M. Dhayal, Ultra small gold nanoparticles synthesis in aqueous solution and their application in fluorometric collagen estimation using bi-ligand functionalisation, *RSC Adv.*, 4, 18250-18256, 2014.
154. W. Haiss, N. T. Thanh, J. Aveyard, D. G. Fernig, Determination of size and concentration of gold nanoparticles from UV-vis spectra, *Anal. Chem.*, 79, 4215-21, 2007.
155. M. Trinadh, K. Govindaraj, T. Rajasekhar, M. Dhayal, A. V. S. Sainath, Synthesis and characterization of poly (ethylene oxide)-based glycopolymers and their biocompatibility with osteoblast cells, *Polym.*, 64(6), 795-803, 2015.
156. M. Trinadh, G. Kannan, T. Rajasekhar, A. V. S. Sainath, M. Dhayal, Synthesis of glycopolymers at various pendant spacer lengths of glucose moiety and their effects on adhesion, viability and proliferation of osteoblast cells, *RSC Adv.*, 4 (70), 37400-37410, 2014.
157. B. Wang, K. Chen, S. Jiang, F. Reincke, W. J. Tong, D. Y. Wang, C. Y. Gao, Chitosan- Mediated Synthesis of Gold Nanoparticles on Patterned Poly (dimethylsiloxane) Surfaces, *Biomacromolecules*, 7, 1203-1209, 2002.
158. M. Rinaudo, Chitin and Chitosan: Properties and Applications, *Prog. Polym. Sci.*, 31, 603-632, 2006.
159. V. Boeris, Y. Micheletto, M. Lionzo, N.P. Da Silveira, G. Pico, Interaction Behavior between chitosan and pepsin, *Carbohydr. Polym.*, 84, 459-464, 2011.
160. L. Jin, R. Bai, Mechanisms of Lead Adsorption on Chitosan/PVA Hydrogel Beads, *Langmuir*, 18, 9765-9770, 2002.
161. S. Jafari, B. Mahyad, H. Heshemzaden, S. Janfaza, T. Gholikhani, et.al., Biomedical Applications of TiO₂ Nanostructures: Recent Advances, *Int. J. Nanomed.*, 15, 3447-3470, 2020.
162. Z. F. Yin, L. Wu, H. G. Yang and Y. H. Su, Recent progress in biomedical applications of titanium dioxide, *Phys. Chem. Chem. Phys.*, 15, 4844-4858, 2013.
163. L. H. Li, Y. M. Kong, H. W. Kim, Y. W. Kim, H. E. Kim, et.al., Improved biological performance of Ti implants due to surface modification by micro-arc oxidation, *Biomaterials*, 25, 2867-2875, 2004.

164. M. Chen, Y. Hu, M. Li, M. Chen, X. Shen, et.al., Regulation of osteoblast differentiation by osteocytes cultured on sclerostin antibody conjugated TiO₂ nanotube array, *Colloids Surf. B: Biointerfaces*, 175, 663-670, 2019.
165. Q. Zhu, X. Li, Z. Fan, Y. Xu, H. Niu, et.al., Biomimetic polyurethane/TiO₂ nanocomposite scaffolds capable of promoting biomineralization and mesenchymal stem cell proliferation, *Mater. Sci. Eng. C*, 85, 79-87, 2018.
166. M. Berridge, A. Tan, K. McCoy, R. Wang, The Biochemical and Cellular Basis of Cell Proliferation Assays that Use Tetrazolium Salts, *Biochemica.*, 4, 14–19, 1996.
167. C. Foglieni, C. Meoni and A. M. Davalli, Fluorescent dyes for cell viability: an application on prefixed conditions, *Histochem. Cell Biol.*, 115, 223–229, 2001.
168. S. Suzuki, J. Namiki, S. Shibata, Y. Mastuzaki, H. Okano, The neural stem/progenitor cell marker nestin is expressed in proliferative endothelial cells, but not in mature vasculature, *J. Histochem. Cytochem.*, 58, 721-730, 2010.
169. A. Kriegstein, and A. Alvarez-Buylla, The glial nature of embryonic and adult neural stem cells, *Annu. Rev. Neurosci.*, 32, 149-84, 2009.
170. Q. Hu, P. Khanna, B. S. E. Wong, Z. S. L Heng, C. S. Subramanyam, et. al., Oxidative stress promotes exit from the stem cell state and spontaneous neural differentiation, *Octotarget*, 9, 4223-4238, 2017.
171. V. S. Adusumilli, T. L. Walker, R. W. Overall, G. M. Klatt, S. A. Zeidan, et.al., ROS Dynamics Delineate Functional States of Hippocampal Neural Stem Cells and Link to Their Activity – Dependent Exit from Quiescence, *Cell Stem Cell*, 28, 300-314.e6, 2021.
172. S. Oka, T. Tsuzuki, M. Hidaka, M. Ohno, Y. Nakatsu, et.al, Endogenous ROS production in early differentiation state suppresses endoderm differentiation via transient FOXC1 expression, *Cell Death Discov.*, 8, 150, 2022.
173. R. T Briggs, D. B. Drath, M. L. Karnovsky, M. J. Karnovsky, Localization of NADH oxidase on the surface of human polymorphonuclear leukocytes by a new cytochemical method, *J. Cell. Biol.*, 67, 566–86, 1975.
174. G. T. Babcock, M. Wikstrom, Oxygen activation and the conservation of energy in cell respiration. *Nature*, 356, 301–309, 1992.
175. E. Margittai, G. Bánhegyi, Oxidative folding in the endoplasmic reticulum: towards a multiple oxidant hypothesis? *FEBS Lett.*, 584, 2995–2998, 2010.
176. J. Aguirre, M. R. Momberg, D. Hewitt, W. Hansberg, Reactive oxygen species and development in microbial eukaryotes, *Trends Microbiol.*, 13, 111–118, 2005.
177. R. Desikan, M. K. Cheung, J. Bright, D. Henson, J. T. Hancock, et.al., ABA, hydrogen peroxide and nitric oxide signalling in stomatal guard cells, *J. Exp. Bot.*, 55, 205–212, 2004.
178. G. Wolf, Role of reactive oxygen species in angiotensin II-mediated renal growth, differentiation, and apoptosis, *Antioxid. Redox Signal*, 7, 1337–1345, 2005.
179. M. Puceat, Role of Rac-GTPase and Reactive Oxygen Species in Cardiac Differentiation of Stem Cells, *Antioxid. Redox Signal*, 7,1435–1439, 2005.
180. H. Kamata, S. i. Oka, Y. Shibukawa, J. Kakuta, H. Hirata, Redox regulation of nerve growth factor-induced neuronal differentiation of PC12 cells through modulation of the nerve growth factor receptor, TrkA, *Arch Biochem. Biophys.*, 434, 16–25, 2005.
181. L. Zhang, G. Wang, X. Chen, X. Xue, Q. Guo, et. al., Formyl peptide receptors promotes neural differentiation in mouse neural stem cells by ROS generation and regulation of PI3K-AKT signaling, *Sci. Rep.*, 7, 206, 2017.

182. J. Y. Lee, M. Y. Chang, C. H. Park, H. Y. Kim, J. H. Kim, et al., Ascorbate-induced differentiation of embryonic cortical precursors into neurons and astrocytes, *J. Neurosci. Res.*, 73, 156–165, 2003.
183. S. J. Morrison, M. Csete, A. K. Groves, W. Melega, B. Wold, et al., Culture in reduced levels of oxygen promotes clonogenic sympathoadrenal differentiation by isolated neural crest stem cells, *J. Neurosci.*, 20, 7370–7376, 2000.
184. J. Smith, E. Ladi, M. Mayer-Proschel, M. Noble, Redox state is a central modulator of the balance between self-renewal and differentiation in a dividing glial precursor cell, *Proc. Natl. Acad. Sci. U S A*, 97, 10032–10037, 2009.
185. R. Domenis, N. Bergamin, G. Gianfranceschi, C. Vascotto, M. Romanello, et al., The redox function of APE1 is involved in the differentiation process of stem cells toward a neuronal cell fate, *PLoS One*, 9, e8923, 2014.
186. J. Aguirre, M. R. Momberg, D. Hewitt, W. Hansberg, Reactive oxygen species and development in microbial eukaryotes, *Trends Microbiol.*, 13, 111–118, 2005.
187. N. Pashkovskaia, U. Gey, G. Rödel, Mitochondrial ROS direct the differentiation of murine pluripotent P19 cells, *Stem Cell Res.*, 30, S180-191, 2018.
188. V. Mathews, P. T. Hanson, E. Ford, J. Fujita, K. S. Polonsky, et al. Recruitment of bone marrow-derived endothelial cells to sites of pancreatic beta-cell injury, *Diabetes* 53, 91-98, 2004.
189. H. Jahr, and R.G. Bretzel, Insulin-positive cells in vitro generated from rat bone marrow stromal cells, *Transplant. Proc.* 35, 2140-2141, 2003.
190. L. B. Chen, X. B. Jian, and L. Yang, Differentiation of rat marrow mesenchymal stem cells into pancreatic islet beta-cells, *World J. Gastroenterol.* 10, 3016-3020, 2004.
191. A. Ianus, G.G. Holz, N. D. Theise, and M. A. Hussain, In vivo derivation of glucose-competent pancreatic endocrine cells from bone marrow without evidence of cell fusion, *J. Clin. Invest.* 111, 843–850, 2003.
192. A. Lechenr, and J. F. Habener, Stem/progenitor cells derived from adult tissues: potential for the treatment of diabetes mellitus, *Am. J. Physiol. Endocrinol. Metab.* 284, E259-66, 2003.
193. K. A. D'Amour, et al. Production of pancreatic hormone-expressing endocrine cells from human embryonic stem cells, *Nat. Biotechnol.* 24, 1392-1401, 2006.
194. A. J. Vegas, et al. Long-term glycemic control using polymer-encapsulated human stem cell-derived beta cells in immune-competent mice, *Nat. Med.* 22, 1-6, 2016.
195. D. Zhang, et al. Highly efficient differentiation of human ES cells and iPS cells into mature pancreatic insulin-producing cells, *Cell Res.* 19, 429-438, 2009.
196. X. F. Hua, et al. Pancreatic insulin-producing cells differentiated from human embryonic stem cells correct hyperglycemia in SCID/NOD mice, An animal model of diabetes, *PLoS One* 9, e102198, 2014.
197. A. S. Lee, C. Tang, M. S. Rao, I. L. Weissman, and J. C. Wu, Tumorigenicity as a clinical hurdle for pluripotent stem cell therapies, *Nat. Med.* 19, 998, 2013.
198. K. English, and K. Wood, Immunogenicity of embryonic stem cell-derived progenitors after transplantation, *Curr. Opin. Organ Transplant.* 16, 90-95, 2011.
199. M. Zalzman, et al. Reversal of hyperglycemia in mice by using human expandable insulin-producing cells differentiated from fetal liver progenitor cells, *Proc. Nat. Acad. Sci. USA.* 100, 7253, 2003.
200. M. S. Rao, et al. Characterization of hepatic progenitors from human fetal liver during second trimester, *World J. Gastroenterol.* 14, 5730-5737, 2008.

201. W. J. Choi, et al. Effects of substrate conductivity on cell morphogenesis and proliferation using tailored, atomic layer deposition-grown ZnO thin films, *Sci. Rep.* 5, 9974, 2015.
202. L.Z.Cao, M.E.Tang, E.H.Marko, L.Shi-Wu, and Y.Li-Jun, High glucose is necessary for complete maturation of pdx 1-VP16-expressing hepatic cells into functional insulin producing cells, *Diabetes* 53, 3168-3178, 2004.
203. S.K.Vishwakarma, et al. In vitro quantitative and relative gene expression analysis of pancreatic transcription factors Pdx-1, Ngn-3, Isl-1, Pax-4, Pax-6 and Nkx-6.1 in trans-differentiated human hepatic progenitors, *J. Diabet. Investig.* 5, 492-500, 2014.
204. A. A. Khan, et al. In Vitro Insulin Production and Analysis of Pancreatic Transcription Factors in Induced Human Hepatic Progenitor Cells, *Diabet. Technol. Ther.* 12, 373-378, 2010a.
205. A. A. Khan, et al. In Vitro Insulin Production and Analysis of Pancreatic Transcription Factors in Induced Human Hepatic Progenitor Cells. Human Fetal Liver-Derived Stem Cell Transplantation as Supportive Modality in the Management of End-Stage Decompensated Liver Cirrhosis, *Cell Transplant.* 19, 409-418, 2010b.
206. Z. Alipio, et al. Reversal of hyperglycemia in diabetic mouse models using induced-pluripotent stem (iPS)-derived pancreatic β -like cells, *PNAS* 107, 13426-13431, 2010b.
207. F. W. Pagliuca, et al. Generation of functional human pancreatic β -cells in vitro, *Cell* 159, 428-439, 2014.
208. O. Veisoh, B. C. Tang, K. A. Whitehead, D. G. Anderson, and R. Langer, Managing diabetes with nanomedicine: challenges and opportunities, *Nat. Rev. Drug. Discov.* 14, 45-47, 2015.
209. H. Nathaniel, D. J. Mooney, Inspiration and application in the evolution of biomaterials, *Nature*, 462, 426-32, 2009.
210. M. P. Lutolf, F. E. Weber, H. G. Schmoekel, J. C. Schense, T. Kohler, et al. Repair of bone defects using synthetic mimetics of collagenous extracellular matrices, *Nat. Biotechnol.* 21:513-18, 2003.
211. J. A. Hubbell, Biomaterials in tissue engineering, *Nat. Biotechnol.* 13:565-76, 1995.
212. Z. You, H. Cao, J. Gao, P. H. Shin, B. W. Day, et al. A functionalizable polyester with free hydroxyl groups and tunable physicochemical and biological properties, *Biomaterials* 31:3129-38, 2010.
213. M. Geetha, A. K. Singh, R. Asokamani, A. K. Gogia, Ti based biomaterials, the ultimate choice for orthopedic implants – A review, *Prog Mater Sci* ;54:397-425, 2009.
214. C. Loty, J. M. Sautier, M. T. Tan, M. Oboeuf, E. Jallot, et al. Bioactive Glass Stimulates In Vitro Osteoblast Differentiation and Creates a Favorable Template for Bone Tissue Formation, *J Bone Miner Res*;16:231–239, 2001.
215. J. Kohn, New approaches to biomaterials design, *Nature Mater.* 3:745-47, 2004.
216. A. Trampuz, A. F. Widmer, Infections associated with orthopedic implants, *Curr Opin. Infect. Dis.* 19:349-56, 2006.
217. K. J. Edgar, C. M. Buchanan, J. S. Debenham, P. A. Rundquist, B. D. Seiler, et al. Advances in cellulose ester performance and application, *Prog. Polym. Sci.*, 26, 1605–1688, 2001.

218. L. Crepy, V. Miri, N. Joly, P. Martin, and J. M. Lefebvre, Effect of side chain length on structure and thermomechanical properties of fully substituted cellulose fatty esters, *Carbohydr. Polym.* 83, 1812–1820, 2011.
219. T. Danjo, T. Iwata, Syntheses of cellulose branched ester derivatives and their properties and structure analyses, *Polymer*, 137, 358–363, 2018.
220. E. T. H. Vink, K. R. Rábago, D. A. Glassner, P. R. Gruber, Application of life cycle assessment to NatureWorks™ polylactide (PLA) production, *Polym. Degrad. Stab.*, 80, 403–419, 2003.
221. R. Auras, B. Harte, S. Selke, An Overview of Polylactides as Packaging Materials, *Macromol. Biosci.*, 4, 835–864, 2004.
222. R. W. Lenz, R. H. Marchessault, Bacterial Polyesters: Biosynthesis, Biodegradable Plastics and Biotechnology, *Biomacromolecules*, 6, 1, 2005.
223. T. Iwata, Strong Fibers and Films of Microbial Polyesters, *Macromol. Biosci.*, 5, 689, 2005.
224. E. M. Malik, C. E. Müller, Anthraquinones as Pharmacological Tools and Drugs, *Medicinal Research Reviews*, 36, 4, 705–748, 2016.
225. A. Gao, H. Zhanga, G. Sun, K. Xie and A. Hou, Light-induced antibacterial and UV-protective properties of polyamide 56 biomaterial modified with anthraquinone and benzophenone derivatives, *Materials & Design*.
226. D. Bradley, G. Williams, M. Lawton., Drying of organic solvents: quantitative evaluation of the efficiency of several desiccants, *J. Org. Chem.* 75, 8351-8354, 2010.
227. C. E. Rehberg, M. B. Dixon, C. H. Fisher, Polymerizable esters of lactic acid A-carbalcoxylethyl acrylates and methylacrylates, *J. Am. Chem. Soc.* 67, 208-210, 1945.
228. M. Trinadh, K. Govindaraj, V. Santosh, M. Dhayal and A. V. S. Sainath, Synthesis of PEO-based di-block glycopolymers at various pendant spacer lengths of glucose moiety and their in-vitro biocompatibility with MC3T3 osteoblast cells, *Des Monomers and Polym.* 19, 24-33, 2016.
229. T. Goto, T. Iwata and H. Abe. Synthesis and Characterization of Biobased Polyesters Containing Anthraquinones Derived from Gallic Acid, *Biomacromolecules*, 20, 318–325, 2019.
230. J. Cao, F. Ding, H. Chen, H. Wang, W. Wang, et al., A new redox-active conjugated polymer containing anthraquinone pendants as anode material for aqueous all-organic hybrid-flow battery, *J. Power Sources*, 423, 316-322, 2019,
231. F. Juvenal, H. Lei, A. Schlachter, P. L. K. Pierre, and D. Harvey., Ultrafast photo-induced electron transfers in platinum (II)-Anthraquinone diimine polymers/PCBM films, *J. Phys. Chem.* 123, 5289-5302, 2019.
232. P. W. Tang, R. Liang, D. L., Qihang Y. H. Jiahui, D. B. Cao, et al. Highly Stable and High Rate-Performance Na-Ion Batteries Using Polyanionic Anthraquinone as the Organic Cathode, *ChemSusChem.*, 12, 2181-2185, 2019.
233. D. K. Patel, and K. T. Lim, Biomimetic Polymer-Based Engineered Scaffolds for Improved Stem Cell Function, *Materials (Basel, Switzerland)*, 12, 2950. 11, 2019.
234. Y. Zhang, R. Meng, J. Zhou, X. Liu, and W. Guo, Halloysite nanotubes-decorated electrospun biobased polyamide scaffolds for tissue engineering applications, *Colloids Surf. A: Physicochem. Eng. Asp.*, 648, 129378, 2022.
235. V. Sarangthem, H. Sharma, M. Mendiratta, R. K. Sahoo, R. W. Park, et al. Application of Bio-Active Elastin-like Polypeptide on Regulation of Human Mesenchymal Stem Cell Behavior, *Biomedicines*. 10, 1151, 2022.

236. N. Zhang, and D. H. Kohn. Using polymeric materials to control stem cell behavior for tissue regeneration, Birth defects research. Part C, *Embryo today : reviews*, 96, 63-81, 2012.
237. A. Varki, Biological roles of oligosaccharides: all of the theories are correct, *Glycobiology*, 3, 97-130, 1993.
238. T. K. Dam, F. C. Brewer, Maintenance of cell surface glycan density by lectin-glycan interactions: A homeostatic and innate immune regulatory mechanism, *Glycobiology*, 20:1061-64, 2010.
239. J. Kohn, New approaches to biomaterials design, *Nature Mater.*, 3:745-47, 2004.
240. B. Valamehr, S. J. Polleux, J. Qiao, R. Guo, S. Gschweng, et al. Hydrophobic surfaces for enhanced differentiation of embryonic stem cell-derived embryoid bodies, *Proceedings of the National Academy of Sciences of the United States of America*, 105, 14459–14464, 2008.
241. S. M. J. Wharton, K. S. Siow, A. Rahman, A. Aminuddin, and P. Y. Ng, Effect of Sulfur on Nitrogen-Containing Plasma Polymers in Promoting Osteogenic Differentiation of Wharton’s Jelly Mesenchymal Stem Cells, *SainsMalaysiana*, 50, 239-251, 2021.
242. Y. Yan, S. Shin, B. S. Jha, Q. Liu, J. Sheng, et al. Efficient and rapid derivation of primitive neural stem cells and generation of brain subtype neurons from human pluripotent stem cells, *Stem Cells Transl. Med.* 2, 862–870, 2013.
243. K. R. Yu, J. H. Shin, J. J. Kim, M. G. Koog, J. Y. Lee, et al. Rapid and Efficient Direct Conversion of Human Adult Somatic Cells into Neural Stem Cells by HMGA2/let-7b. *Cell Rep.*, 10, 441–452, 2015.
244. A. Shahbazi, M. Safa, F. Alikarami, S. Kargozar, M. H. Asadi, et al. Rapid Induction of Neural Differentiation in Human Umbilical Cord Matrix Mesenchymal Stem Cells by cAMP-elevating Agents, *Int. J. Mol. Cell. Med.* 5, 167–177, 2016.
245. J. Lu, L. C. D. Bovi, J. Hecht, R. Folkerth, and V. L. Sheen, Generation of neural stem cells from discarded human fetal cortical tissue, *J. Vis. Exp.*, 51, e2681, 2011.
246. X. Duan, E. Kang, C. Y. Liu, G. L. Ming, and H. Song, Development of neural stem cell in the adult brain, *Curr. Opin. Neurobiol.* 18, 108–115, 2008.
247. K. R. Yu, J. H. Shin, J. J. Kim, M. G. Koog, J. Y. Lee, et al., Rapid and Efficient Direct Conversion of Human Adult Somatic Cells into Neural Stem Cells by HMGA2/let-7b, *Cell Rep.*, 10, 441–452, 2015.
248. Y. Yan, S. Shin, B. S. Jha, Q. Liu, J. Sheng, et al., Efficient and rapid derivation of primitive neural stem cells and generation of brain subtype neurons from human pluripotent stem cells, *Stem Cells Transl. Med.*, 2, 862–870, 2013.
249. Y. Tang, P. Yu, L. Cheng, Current progress in the derivation and therapeutic application of neural stem cells, *Cell Death Dis.* 8, e3108, 2017.
250. S. Casarosa, Y. Bozzi, L. Conti, Neural stem cells: Ready for therapeutic applications?, *Mol. Cell. Ther.*, 2014.
251. S. E. Marsh, M. B. Jones, Neural stem cell therapy for neurodegenerative disorders: The role of neurotrophic support, *Neurochem. Int.*, 106, 94–100, 2017.
252. C. B. Low, Y. C. Liou, B. L. Tang, Neural differentiation and potential use of stem cells from the human umbilical cord for central nervous system transplantation therapy, *J. Neurosci. Res.* 86, 1670–1679, 2008.

253. J. Lu, L. C. D. Bovi, J. Hecht, R. Folkert, and V. L. Sheen, Generation of neural stem cells from discarded human fetal cortical tissue, *J. Vis. Exp.*, 51, e2681, 2011.
254. X. Duan, E. Kang, C. Y. Liu, G.L. Ming, H. Song, Development of neural stem cell in the adult brain, *Curr. Opin. Neurobiol.*, 18, 108–115, 2008.
255. S. Casarosa, Y. Bozzi, L. Conti, Neural stem cells: Ready for therapeutic applications?, *Mol. Cell. Ther.*, 2, 31, 2014.
256. L. Fu, L. Zhu, Y. Huang, T. D. Lee, S. J. Forman, et al. Derivation of neural stem cells from mesenchymal stem cells: Evidence for a bipotential stem cell population, *Stem Cells Dev.* 17, 1109–1121, 2008.
257. J. Jaiswal, M. Dhayal, Electrochemically differentiated human MSCs biosensing platform for quantification of nestin and β -III tubulin as whole-cell system, *Biosens. Bioelectron.* 206, 114134, 2022.
258. J. M. Gimble, F. Guilak, M. E. Nuttall, S. Sathishkumar, M. Vidal, et al. In vitro Differentiation Potential of Mesenchymal Stem Cells. *Transfus. Med. Hemother.* 35, 228–238, 2008.
259. L. Jackson, D. R. Jones, P. Scotting, V. Sottile, Adult mesenchymal stem cells: Differentiation potential and therapeutic applications, *J. Postgrad. Med.* 53, 121–127, 2007.
260. K. Ma, L. Fox, G. Shi, J. Shen, Q. Liu, et al., Generation of neural stem cell-like cells from bone marrow-derived human mesenchymal stem cells, *Neurol. Res.* 33, 1083–1093, 2011.
261. A. R. Alexanian, An efficient method for generation of neural-like cells from adult human bone marrow-derived mesenchymal stem cells, *Regen. Med.* 5, 891–900, 2010.
262. S. Chen, W. Zhang, J. M. Wang, H. T. Duan, J. H. Kong, et al., Differentiation of isolated human umbilical cord mesenchymal stem cells into neural stem cells, *Int. J. Ophthalmol.* 9, 41–47, 2010.
263. C. Leite, N. T. Silva, S. Mendes, A. Ribeiro, J. P. D. Faria, et al., Differentiation of human umbilical cord matrix mesenchymal stem cells into neural-like progenitor cells and maturation into an oligodendroglial-like lineage, *PLoS ONE*, 2014
264. M. Messerli, A. Wagner, R. Sager, M. Mueller, M. Baumann, D.V. Surbek, A. Schoeberlein, Stem cells from umbilical cord Wharton’s jelly from preterm birth have neuroglial differentiation potential, *Reprod. Sci.* 20, 1455–1464, 2013.
265. J. B. Jensen, M. Parmar, Strengths and limitations of the neurosphere culture system, *Mol. Neurobiol.*, 34, 153–161, 2006.
266. J. Du, C. Agatemor, C. T. Saeui, R. Bhattacharya, X. Jia, K.J.Yarema, Glycoengineering Human Neural and Adipose Stem Cells with Novel Thiol-Modified N-Acetylmannosamine (ManNAc) Analogs, *Cells.* Feb 12;10, 377, 2021.
267. A. Farrukh, S. Zhao and A. D. Campo, Microenvironments Designed to Support Growth and Function of Neuronal Cells, *Frontiers in Materials*, 5, 1-22, 2018.
268. D. P. Dowling, I. S Miller, M. Ardhaoui, W. M. Gallagher, Effect of surface wettability and topography on the adhesion of osteosarcoma cells on plasma-modified polystyrene, *J Biomater Appl.*, 26(3), 327-47, 2011.
269. C. Shuxiang, W. C. Yang, W. Liang, W. Y. Haibo and L. Liu, Recent advance in surface modification for regulating cell adhesion and behaviors, *Nanotechno. Rev.*, 9, , 971-989, 2020.

270. W. Song and J. F. Mano, Interactions between cells or proteins and surfaces exhibiting extreme wettabilities, *Soft Matter*, 11, 2013.
271. M. Dhayal, R. Kapoor, P. G. Sistla, R. R. Pandey, S. Kar, et al. Strategies to prepare TiO₂ thin films, doped with transition metal ions, that exhibit specific physicochemical properties to support osteoblast cell adhesion and proliferation, *Materials Science and Engineering C* 37, 99-107, 2014.
272. M. Trinadh, K. Govindaraj, T. Rajasekhar, M. Dhayal, and A. V. Sainath, Synthesis and characterization of poly (ethylene oxide) based glycopolymers and their biocompatibility with osteoblast cells, *Polymer International*, 64 (6), 795-803, 2015.
273. J. S. Francisco, S. Valdez, L. F. Quintero, A. Patricio, Z. Morin, et al. The Influence of Non Polar and Polar Molecules in Mouse Motile Cells Membranes and Pure Lipid Bilayers, *Plos One*, 2013.
274. M. Trinadh, G. Kannan, T. Rajasekhar, A. V. S. Sainath, and M Dhayal ,Synthesis of glycopolymers at various pendant spacer lengths of glucose moiety and their effects on adhesion, viability and proliferation of osteoblast cells, *RSC advances* 4 (70), 37400-37410, 2014.
275. B. C. Heng, S. Jiang, B. Yi, T. Gong, L. W. Lim, and C. Zhang, Small molecules enhance neurogenic differentiation of dental-derived adult stem cells, *Archives of oral biology*, 102, 26–38, 2019.
276. D. G. Nicholls, Mitochondrial membrane potential and aging, *Aging cell* 3, 35–40, 2004.
277. Y. Chen, K. Liu, Y. Shi, and C. Shao, The tango of ROS and p53 in tissue stem cells, *Cell Death Differ.*, 25, 639–641, 2018.
278. N. Spitzer, Electrical activity in early neuronal development, *Nature* 444, 707–712 ,2006.
279. R. Zhu, Z. Sun, C. Li, S. Ramakrishna, K. Chiu, Electrical stimulation affects neural stem cell fate and function in vitro, *Exp. Neurol.* 319, 112963 ,2019.
280. L. He, Z. Sun, J. Li, R. Zhu, B. Niu, et al. Electrical stimulation at nanoscale topography boosts neural stem cell neurogenesis through the enhancement of autophagy signaling, *Biomaterials* 268, 120585 ,2021.
281. M. Hu, L. Hong, C. Liu, S. Hong, S. He, et al. Electrical stimulation enhances neuronal cell activity mediated by Schwann cell derived exosomes, *Sci. Rep.* 9, 4206 ,2019.
282. F. Pires, Q. Ferreira, C. A. V. Rodrigues, J. Morgado, F. C. Ferreira, Neural stem cell differentiation by electrical stimulation using a cross-linked PEDOT substrate: Expanding the use of biocompatible conjugated conductive polymers for neural tissue engineering, *Biochim.Biophys. Acta* 1850, 1158–1168 ,2015.
283. R. Balint, N. J. Cassidy, S. H. Cartmell, Electrical stimulation: a novel tool for tissue engineering, *Tissue Eng. Part B Rev.* 191, 48–57 ,2013.
284. J. Jaiswal, M. Dhayal, Electrochemically differentiated human MSC biosensing platform for quantification of nestin and β -III tubulin as whole-cell system, *Biosens. Bioelectron.* 114134.
285. J. H. Lim, S. D. McCullen, J. A. Piedrahita, E. G. Lobo, N. J. Olby, Alternating current electric fields of varying frequencies: effects on proliferation and differentiation of porcine neural progenitor cells, *Cell. Reprogram.* 15, 405–412 ,2013.
286. W. F. Bai, W. C. Xu, Y. Feng, H. Huang, X. P. Li , et al. Fifty-Hertz electromagnetic fields facilitate the induction of rat bone mesenchymal stromal cells to differentiate into functional neurons, *Cytotherapy* 15, 961–970 ,2013.

287. D. A. Balikov, B. Fang, Y. W. Chun, S. W. Crowder, D. Prasai, et al. Directing lineage specification of human mesenchymal stem cells by decoupling electrical stimulation and physical patterning on unmodified graphene, *Nanoscale* 8, 13730-13739 ,2016.
288. W. Jing, Y. Zhang, Q. Cai, G. Chen, L. Wang, et al. Study of Electrical Stimulation with Different Electric-Field Intensities in the Regulation of the Differentiation of PC12 Cells, *ACS Chem. Neurosci.* 10, 348–357 ,2019.
289. K. A. Chang, J. W. Kim, J. A. Kim, S. E. Lee, S. Kim, et al. Biphasic electrical currents stimulation promotes both proliferation and differentiation of fetal neural stem cells, *PLoS one* 6, e18738 ,2011.
290. G. Thirivikraman, G. Madras, B. Basu, Intermittent electrical stimuli for guidance of human mesenchymal stem cell lineage commitment towards neural-like cells on electroconductive substrates, *Biomaterials* 35, 6219–6235 ,2014.
291. Z. Y. Dong, Z. Pei, Y. L. Wang, Z. Li , Ascl1 Regulates Electric Field-Induced Neuronal Differentiation Through PI3K/Akt Pathway, *Neuroscience* 404, 141–152 ,2019.
292. N.Wang , Xu Yao, T. Qin, F.P.Wang, et al. Myocardin-related transcription factor-A is a key regulator in retinoic acid-induced neural-like differentiation of adult bone marrow-derived mesenchymal stem cell, *Gene* 523, 178-186, 2013.
293. R.S.Jacob, S.Das, D.Ghosh, and S.K. Maji, Influence of retinoic acid on mesenchymal stem cell differentiation in amyloid hydrogels, *Data in Brief* 5, 954–958 , 2015.
294. A.Illendula, N.Fultang, and B.Peethambaran, Retinoic acid induces differentiation in neuroblastoma via ROR1 by modulating retinoic acid response elements, *Oncology Reports* 44, 1013-1024 , 2020.
295. F. Scialo, D. J. Fernández-Ayala, A. Sanz, Role of Mitochondrial Reverse Electron Transport in ROS Signaling: Potential Roles in Health and Disease, *Front Physiol.* 8, 428 ,2017.
296. V. Raimondi, F. Ciccarese, V. Ciminale, Oncogenic pathways and the electron transport chain: a dangerROS liaison, *Br. J. Cancer.* 122, 168-181 ,2020.
297. L. D. Zorova, V. A. Popkov, E. Y. Plotnikov, et al. Mitochondrial membrane potential, *Anal Biochem*, 552, 50-59 ,2018.
298. A. A. Gerencser, C. Chinopoulos, M. J. Birket, M. Jastroch, et al. Quantitative measurement of mitochondrial membrane potential in cultured cells: calcium-induced de- and hyperpolarization of neuronal mitochondria, *J Physiol* 590, 2845-2871 , 2012.
299. H. L. Vieira, P. M. Alves, A. Vercelli, Modulation of neuronal stem cell differentiation by hypoxia and reactive oxygen species, *Prog. Neurobiol.* 93, 444–455,2011.
300. M. Tsatmali, E. C. Walcott, K. L. Crossin, Newborn neurons acquire high levels of reactive oxygen species and increased mitochondrial proteins upon differentiation from progenitors, *Brain Res.* 1040, 137–150 ,2005.
301. W. Jing, Y. Zhang, Q. Cai, G. Chen, et al. Study of Electrical Stimulation with Different Electric-Field Intensities in the Regulation of the Differentiation of PC12 Cells, *ACS Chem. Neurosci.* 10, 348–357 ,2019.
302. A. Nugud, D. Sandeep, A. T. El-Serafi, Two faces of the coin: Minireview for dissecting the role of reactive oxygen species in stem cell potency and lineage commitment, *J. Adv. Res.* 14, 73–79 ,2018.

303. J. E. Park, Y. K. Seo, H. H. Yoon, et al. Electromagnetic fields induce neural differentiation of human bone marrow derived mesenchymal stem cells via ROS mediated EGFR activation, *Neurochem. Int.* 62, 418–424 ,2013.
304. Y. Chen, K. Liu, Y. Shi, C. Shao, The tango of ROS and p53 in tissue stem cells, *Cell Death Differ.* 25, 639–641 ,2018.
305. Eva Correia-Álvarez, James E Keating, Gary Glish, Robert Tarran, M Flori Sassano, Reactive Oxygen Species, Mitochondrial Membrane Potential, and Cellular Membrane Potential Are Predictors of E-Liquid Induced Cellular Toxicity, *Nicotine & Tobacco Research*, Volume 22, 2020, Pages S4–S13,
306. J. M. Suski, M. Lebiezinska, M. Bonora, P. Pinton, et al. Relation between mitochondrial membrane potential and ROS formation, *Methods Mol. Biol.* 810, 183-205 ,2012.
307. H. Liu, Z. He, S. L. April, M. P. Trefny, J. S. Rougier, et al. Biochemical re-programming of human dermal stem cells to neurons by increasing mitochondrial membrane potential, *Cell Death Differ.* 26, 1048-1061 ,2019.
308. A. D. Ducray, A. Felser, J. Zielinski, A. Bittner, J. V. Burgi, et al. Effects of silica nanoparticle exposure on mitochondrial function during neuronal differentiation, *J. Nanobiotechnology* 15, 49 ,2017.
309. J. Augustyniak, J. Lenart, M. Zychowicz, P. P. Stepien, L. Buzanska, Mitochondrial biogenesis and neural differentiation of human iPSC is modulated by idebenone in a developmental stage-dependent manner, *Biogerontology* 18, 665-677,2017.
310. M. Khacho, A. Clark, D. S. Svoboda, J. Azzi, J. G. MacLaurin, et al. Mitochondrial Dynamics Impacts Stem Cell Identity and Fate Decisions by Regulating a Nuclear Transcriptional Program, *Cell Stem Cell* 19, 232-247 ,2016.
311. A. Bahat, A. Gross, Mitochondrial plasticity in cell fate regulation, *J. Biol. Chem.* 294, 13852-13863 ,2019.
312. P. P. Praharaj, B. S. Patro, S. K. Bhutia, Dysregulation of mitophagy and mitochondrial homeostasis in cancer stem cells: Novel mechanism for anti-cancer stem cell-targeted cancer therapy, *Br J Pharmacol.* ,2021.
313. M. K. Paul, B. Bisht, D. O. Darmawan, R. Chiou, et al. Dynamic changes in intracellular ROS levels regulate airway basal stem cell homeostasis through Nrf2-dependent Notch signaling, *Cell Stem Cell.* 15, 199-214 ,2014.
314. K. Wang, T. Zhang, Q. Dong, E. C. Nice, C. Huang, Y. Wei, Redox homeostasis: the linchpin in stem cell self-renewal and differentiation, *Cell Death Dis.* 4, 2013.

Annexure I

Materials and Methods Details

Reagents and materials

Bone marrow-derived human mesenchymal stem cells (hMSCs) and their specific culture media were purchased from Lonza (USA). Indium tin oxide (ITO) coated glass plates (50 mm × 50 mm) were supplied by S. K. Novel Materials & Technologies LLP, New Delhi, India. Polydimethylsiloxane (PDMS) elastomer (Sylgard 184) was brought from Dow Corning. 3-(4,5-dimethyl thiazolyl-2-yl)-2,5-diphenyltetrazolium bromide (MTT), propidium iodide (PI), Hoechst 33342 and paraformaldehyde solution (4%) were acquired from HiMedia, Mumbai, India. Dichlorodihydrofluorescein diacetate (DCFH-DA), all trans-retinoic acid (RA) and 5,5',6,6'-tetrachloro-1,1',3,3'-tetraethyl benzimidazolyl carbocyanine iodide (JC-1) were purchased from Sigma-Aldrich. Monoclonal primary antibodies (mouse anti-nestin and rabbit anti- β -III tubulin) and secondary antibodies (goat anti-mouse IgG Alexa Fluor 594 and goat anti-rabbit IgG Alexa Fluor 488) were from Cell Signaling Technology (USA). All the antibodies were reactive against human antigens and dilutions were done according to recommended manufacturer protocol. All the electrochemical measurement were measured using ZIVE SP1 electrochemical workstation (ZIVE LAB, Seoul, South Korea).

MTT Assay

In-vitro cytotoxicity assessment was performed by MTT assay. The viable cells at the density of 5×10^4 were seeded on coated and uncoated glass chips (control). The cell viability was evaluated after 24 h while cell proliferation was studied for five days. The cell culture media was changed every three days. MTT assay is a simple calorimetric method used for quantification of reduction of yellow coloured tetrazolium salt to purple formazan crystals by metabolically active cells through mitochondrial dehydrogenase enzyme activity []. After specified time interval, the culture medium was removed from each well and 360 μ l of complete medium along with 40 μ l MTT (2 mg/ml in PBS, pH 7.4) solution was added to each well and further incubated for 4 h at 37°C. After incubation, the media was removed completely from each well without disturbing the formed formazan crystals and then solubilized by the addition of dimethyl sulfoxide (DMSO, HiMedia) solution for 30 min. The optical absorbance was read at 570 nm by a microplate reader (Synergy H1 hybrid, Biotek, USA) and the percent cell viability was calculated as the percentage of absorbance of cells seeded on chips in comparison to absorbance of control cells [Gurunathan et al., 2013]. Three independent experiments in triplicates were performed for testing the biocompatibility of coated chips relative to control.

Hoechst 33342 /PI assay

Hoechst 33342/PI dual staining was performed to simultaneously visualise the viable and dead cells seeded on different chips and control for successive days 1, 3, 5 and 7[]. Hoechst 33342, cell permeable nuclear dye, binds to DNA of both viable and non-viable cells. In contrast, the red fluorescent PI, a cell impermeable dye, stains the cells which are dead. The cells were seeded and maintained as described above. After specified period, the depleted media was discarded and cells were washed twice with PBS. Subsequently cells-laden chips and control were stained with Hoechst 33342 (1 μ g mL⁻¹) and PI (1 μ g mL⁻¹) solutions and incubated for 30 min at 37°C in the dark. The cells were finally washed with PBS and images were taken

using an inverted fluorescence microscope (Nikon Eclipse 90i) in blue and red channels as well as in phase contrast.

Immunocytochemistry

The cells at a density of 3×10^4 were cultured on coated chips and control for seven days. After the specified time of culture, the cells were washed with PBS and fixed with 4% paraformaldehyde for 15 min at room temperature. Cells were rinsed further three times with PBS 5 min each. Then the fixed chips were blocked in blocking buffer (0.3% Triton X-100 and 5% normal goat serum in PBS) for 60 min. Subsequently, the blocking buffer was aspirated and chips were incubated with diluted primary antibody (mouse anti-Nestin, 1:3200, rabbit anti- β tubulin-III, 1:300 and mouse anti-GFAP IgG 1:3000) overnight at 4°C. After incubation, washing was done and diluted secondary antibody (1:1000) was added to chips for 2 h at room temperature protected from light, followed by Hoechst staining for cell nuclei. The images were captured using an inverted fluorescence microscope (Nikon Eclipse 90i).

Assessment of mitochondrial membrane potential

The hMSC cells at density of 3×10^4 were seeded on coated and uncoated glass chips (control). The mitochondrial membrane potential (MMP), was evaluated using JC-1 at different days (day 1 to day 7). The seeded cells were washed once with cold PBS and incubated with JC-1 dye (2 μ M) for 20 min in dark at 37°C. The supernatant was removed and cells were washed twice with PBS and pictured immediately using a fluorescence microscope (Nikon Eclipse 90i).

Quantification of intracellular ROS generation

The healthy viable hMSC cells are harvested and seeded at 3×10^4 on coated and uncoated glass chips (control). Three independent experiments were performed for ROS estimation. The cells were maintained following the above mentioned protocol till seven days of cell culture. At desired time points, cells were washed twice and working solution of 10 μ M DCFH-DA in PBS was instilled into each well for 30 min at 37°C in the dark. Afterward, the cells seeded chips and control were washed with PBS and subjected to an inverted fluorescence microscope to visualize the DCF green signals.

The intracellular ROS was quantitatively measured in fluorescence mode of the microplate reader. The cells were seeded on different substrates (1×1 cm²) and control at a density of 5×10^3 cells in a 24-well plate. After 24 h of seeding, the media was discarded and cell-laden substrates were gently washed with PBS (1x) twice. Afterward, 10 μ M DCFH-DA in PBS was added to each well for 45 min at 37°C in the dark. Now the dye was decanted and the cells were washed with PBS. Subsequently, the cells were trypsinized using Trypsin-EDTA and the cell suspension was collected and centrifuged for 1200g for 10 min. Further, the supernatant was discarded and the pellet was resuspended in PBS. 100 μ l of dye-loaded cells were added in a 96-well black and transparent bottom plate. The fluorescence reading was recorded with excitation and emission wavelength at 485 nm and 530 nm, respectively.

Retinoic acid stimulation

The effect of RA on differentiation of hMSCs towards neuronal lineage was studied and compared with the proposed approach of electrostimulating the stem cells for driving neuronal differentiation. hMSCs of cell density 1×10^4 were seeded onto ITO surface for 24 h at 37°C. Afterwards, the seeded hMSCs were incubated with 20 μ M, 10 μ M, 5 μ M, 1 μ M and 0.5 μ M RA in growth medium with a final DMSO concentration of 0.1% (v/v). The RA stimulated

hMSCs were imaged on day 1, 3 and 7 using fluorescence microscope and expression of neural markers, nestin and β -III tubulin, were quantified by performing immunocytochemistry.

Morphological changes using scanning electron microscopy

Scanning electron microscopy (SEM) was used to image the morphology of the hMSCs before and after receiving electrical stimulation. For the analysis, samples were prepared by gently washing the cells adherent platforms with PBS and fixing them in 4% paraformaldehyde solution for 15 min. Then, the solution was poured out, followed by washing and finally dehydrating them by dipping in solutions of 30%, 50%, 70%, 80%, 90%, and 100% ethanol. The prepared platforms were air-dried and imaged without gold coating.

Anexture II

Synthesis of Poly(acryl-1-aminoanthraquinone) conjugated with Maltose-based Segment

Description of Synthesis: The chemical structures of the synthesized polymers were confirmed by FT-IR, ^1H - and ^{13}C -NMR spectroscopic methods. In the PANT FT-IR spectrum, the presence of $-\text{NH}-\text{C}=\text{O}-$ group along with aromatic $-\text{C}=\text{C}-$ symmetric stretchings appeared at 1674 cm^{-1} and 1586 and 1516 cm^{-1} (Figures A7), respectively. In the PANT ^1H -NMR spectrum, the chemical shifts appeared at 2.7 - 0.9 ppm due to RAFT agent moieties at the terminal end of the polymer chain, the characteristic amide $-\text{NH}$ proton appeared at 9.2 to 9.35 ppm and anthraquinone pendent aromatic protons and benzene protons from RAFT agent appeared at 5.9 to 8.4 ppm as given (Figure A8). In the ^{13}C -NMR spectrum, amide carbonyl carbon showed at 165 ppm and aromatic carbons of the PANT appeared in the range of 115 - 142 ppm (Figures A9). The PANT-*b*-PMAM copolymer of FT-IR spectrum showed characteristic ester $\text{O}-\text{C}=\text{O}$ -peak from PMAM block at 1756 cm^{-1} and PANT $-\text{NH}-\text{C}=\text{O}-$ group signal appeared at 1674 cm^{-1} (Figures A7). In the ^1H -NMR spectrum, pendent maltose signals appeared in the range of 5.5 - 3.6 ppm and 8.4 - 7.2 ppm due to anthraquinone pendent aromatic protons (Figures A10). On the other hand, the ^{13}C -NMR spectrum of the copolymer showed signals at 55 - 70 ppm due to the maltose pendent of the PMAM segment along with PANT block signals (Figures A11). Calculated molecular weight values (PANT: 4434 , PANT-*b*-PMAM: 8985 and PMAM: 8148 Da) from the ^1H -NMR spectra and SEC studies values of the weight average molecular weights (M_w) (PANT: 3562 , Đ : 1.1 ; PANT-*b*-PMAM: 11319 , Đ : 1.4 and PMAM: 7811 Da, Đ : 1.2) of the polymers and their polydispersities (Đ) are witnessed in annexure 1, Table A1. The molecular weight values of the polymers from SEC studies and calculation from ^1H -NMR spectra were dissimilar from each other. These dissimilarities may be due to the bulky anthraquinone and pendant acetylated maltose moieties of the polymer chains which hold dissimilarities in hydrodynamic volume compared to the polystyrene standards.

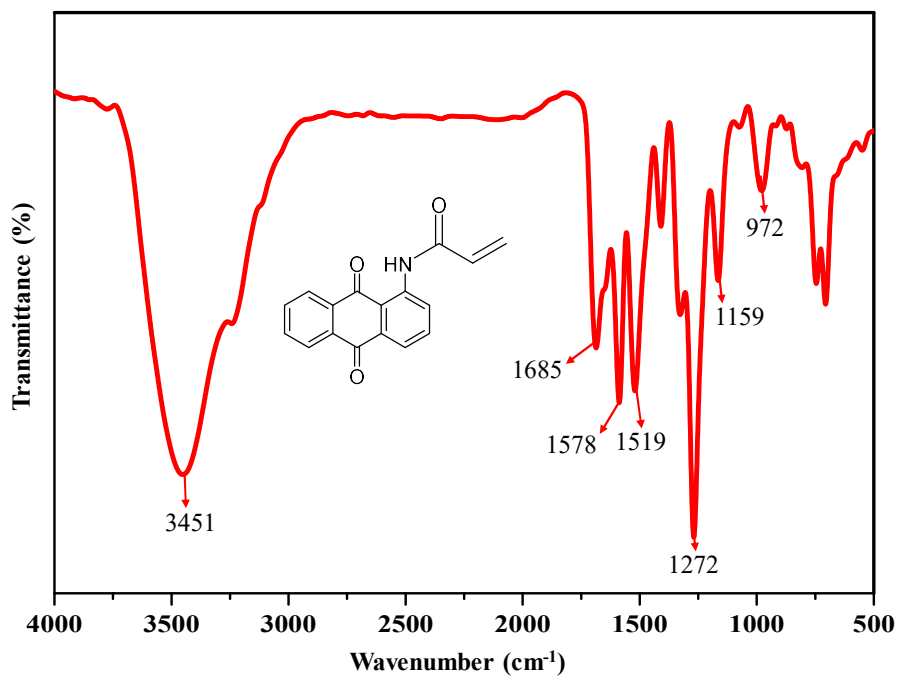


Figure A1. IR spectrum of the ANT monomer.

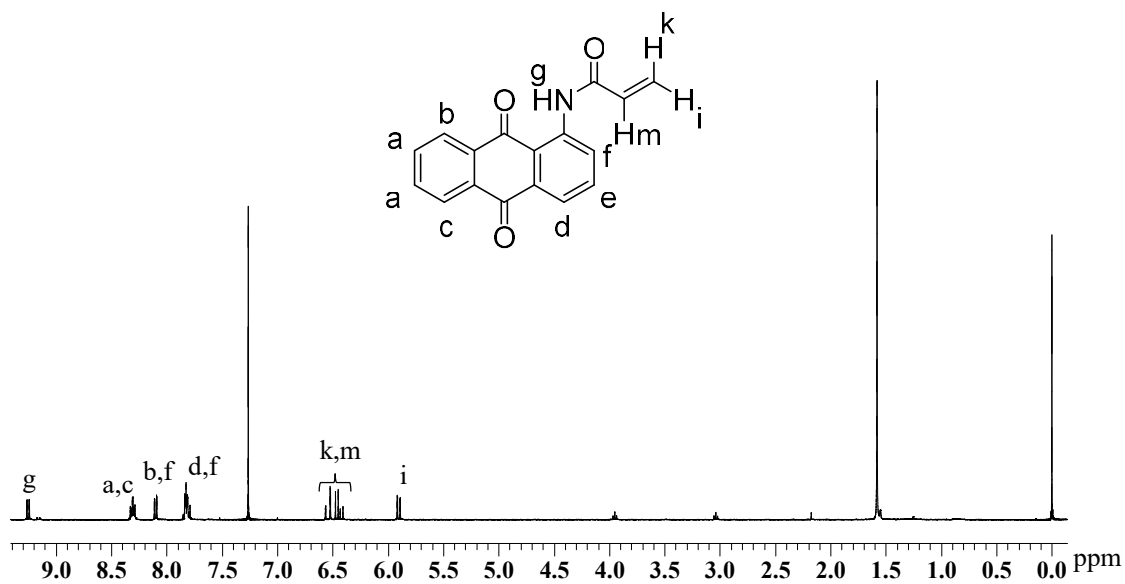


Figure A2. ¹H-NMR spectrum of the ANT monomer.

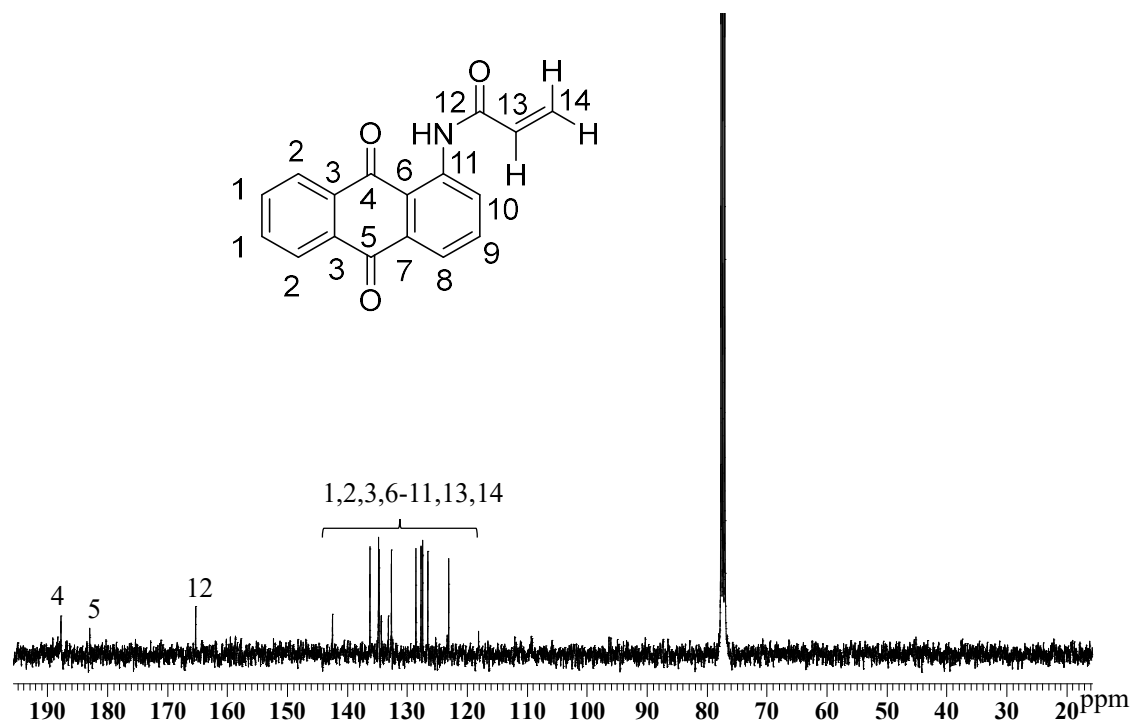


Figure A3. ¹³C-NMR spectrum of the ANT monomer.

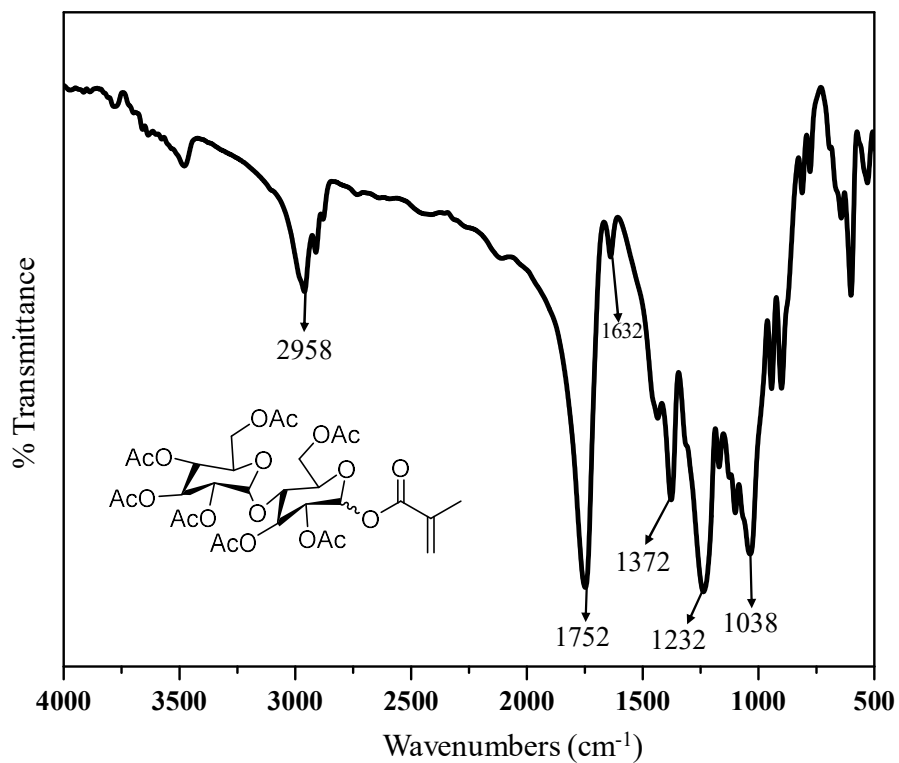


Figure A4. IR spectrum of the MAM monomer.

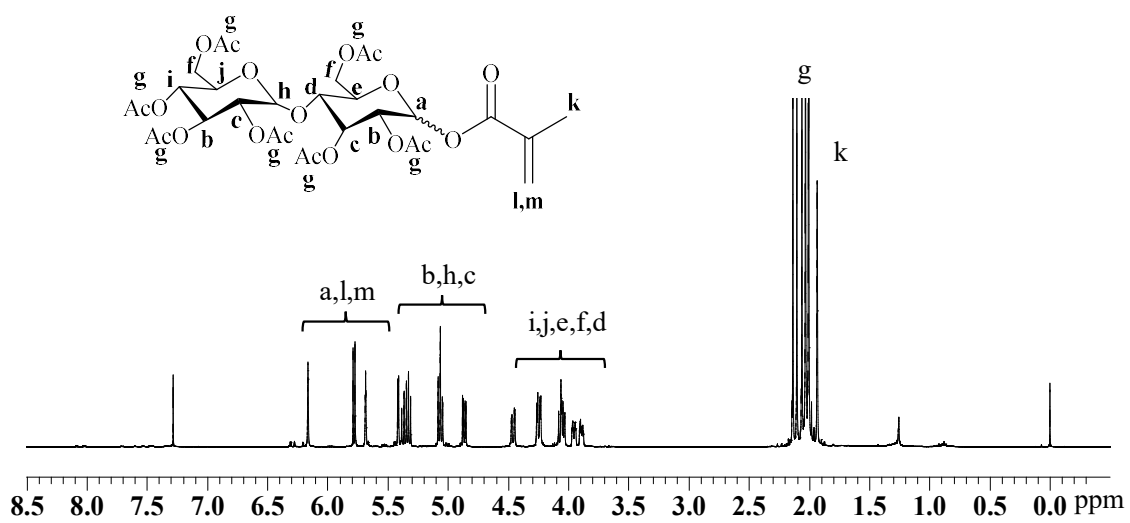


Figure A5. ¹H-NMR spectrum of the MAM monomer.

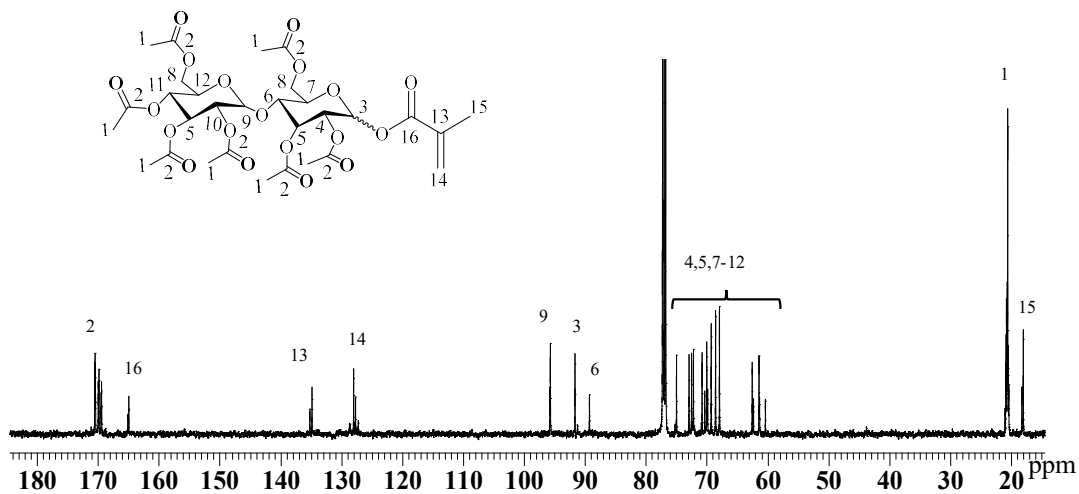


Figure A6. ^{13}C -NMR spectrum of the MAM monomer.

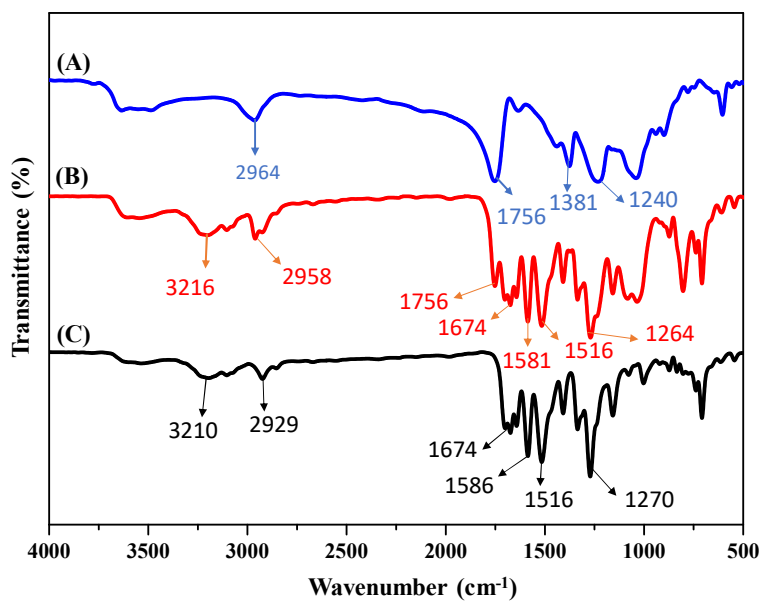


Figure A7. IR spectra of the (A) PMAM, (B) PANT-*b*-PMAM and (C) PANT.

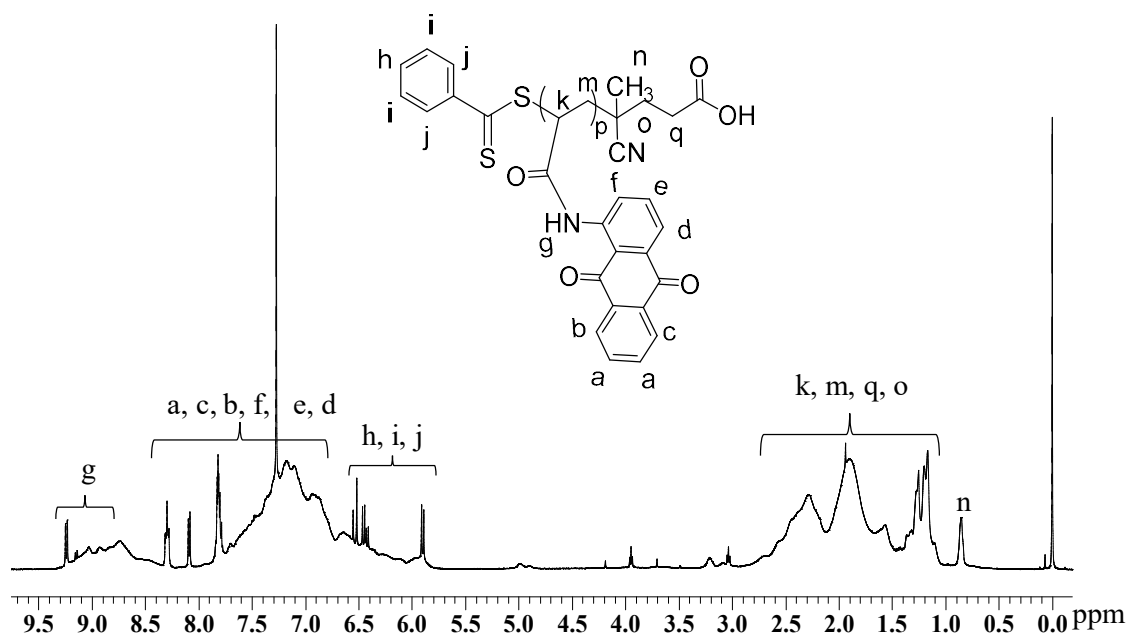


Figure A8. ¹H-NMR spectrum of the PANT homopolymer.

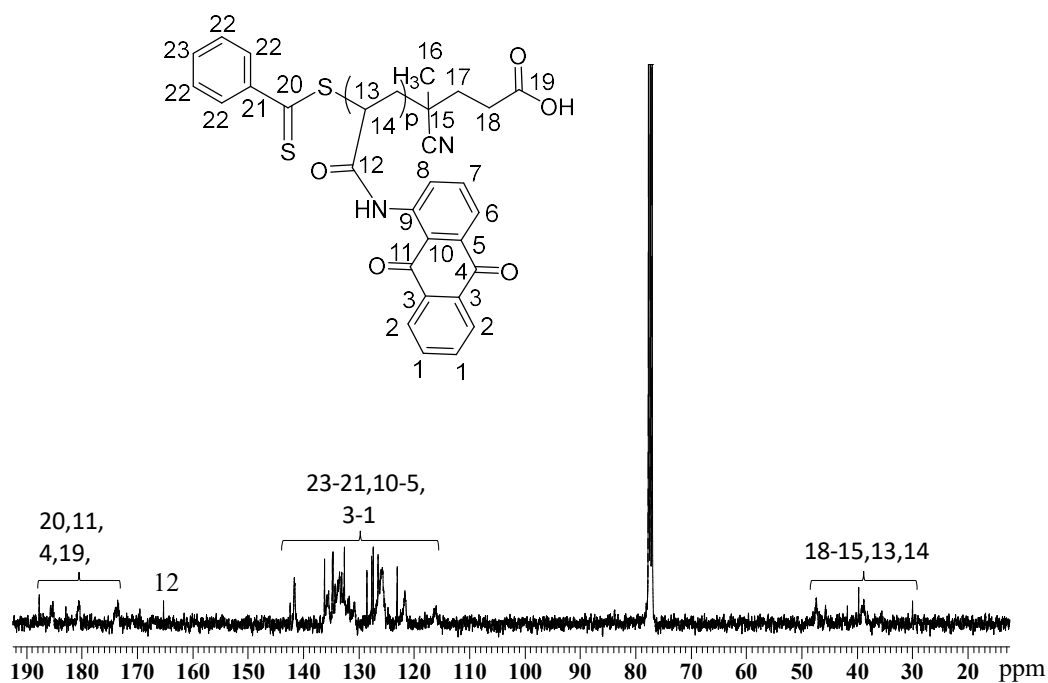


Figure A9. ^{13}C -NMR spectrum of the PANT homopolymer.

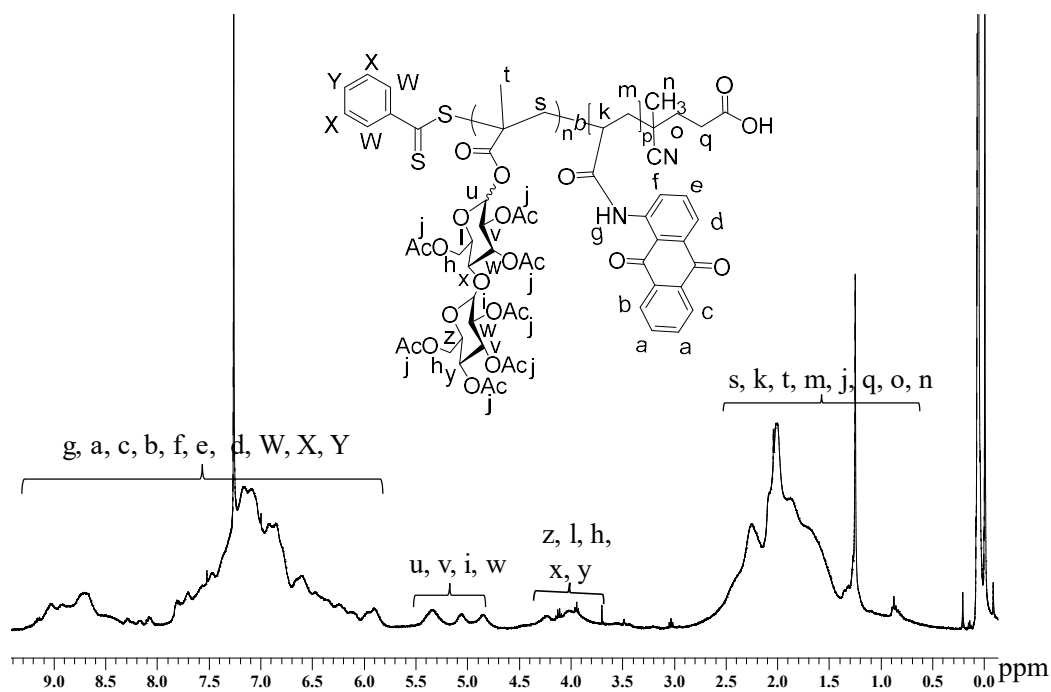


Figure A10. ^1H -NMR spectrum of the PANT-*b*-PMAM di-block copolymer.

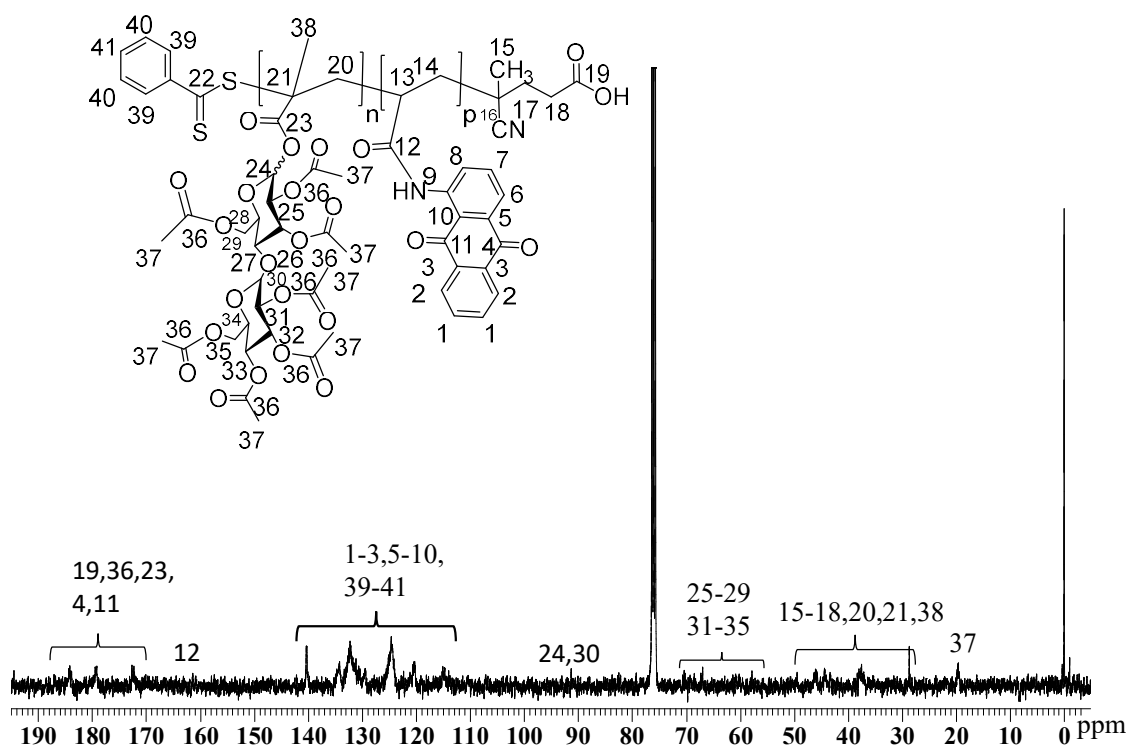


Figure A11. ^{13}C -NMR spectrum of the PANT-*b*-PMAM di-block copolymer.

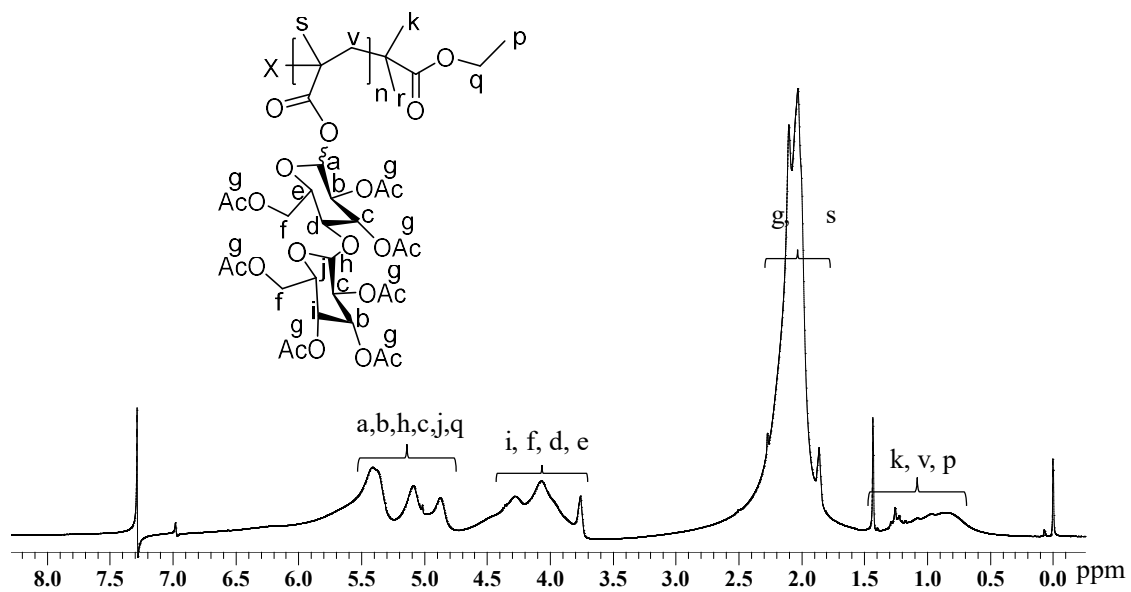


Figure A12. ^1H -NMR spectrum of the PMAM homopolymer.

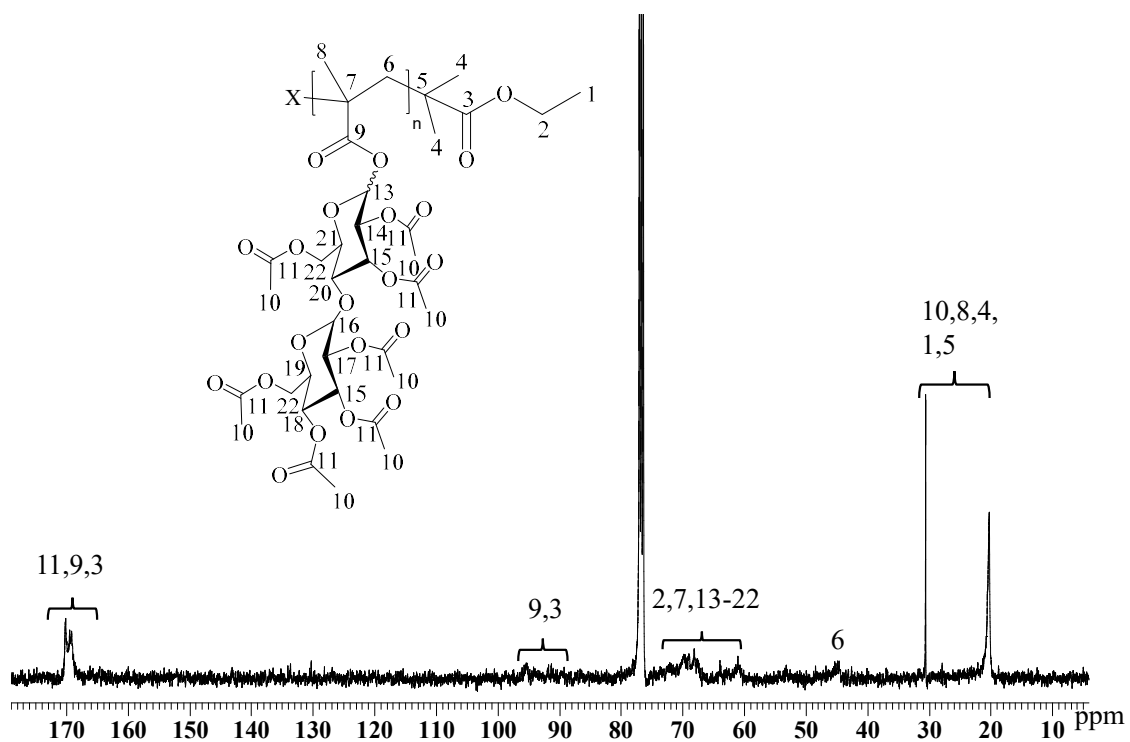


Figure A13. ^{13}C -NMR spectrum of the PMAM homopolymer.

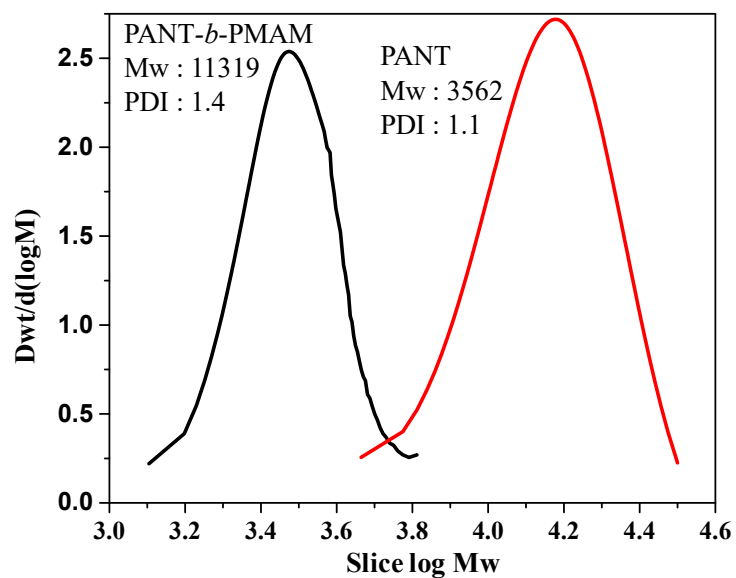


Figure A14. SEC curves of (a) PANT and PANT-*b*-PMAM using injection volume: 20 μL , run time: 40 min and set name: 241017 PS_DMF.

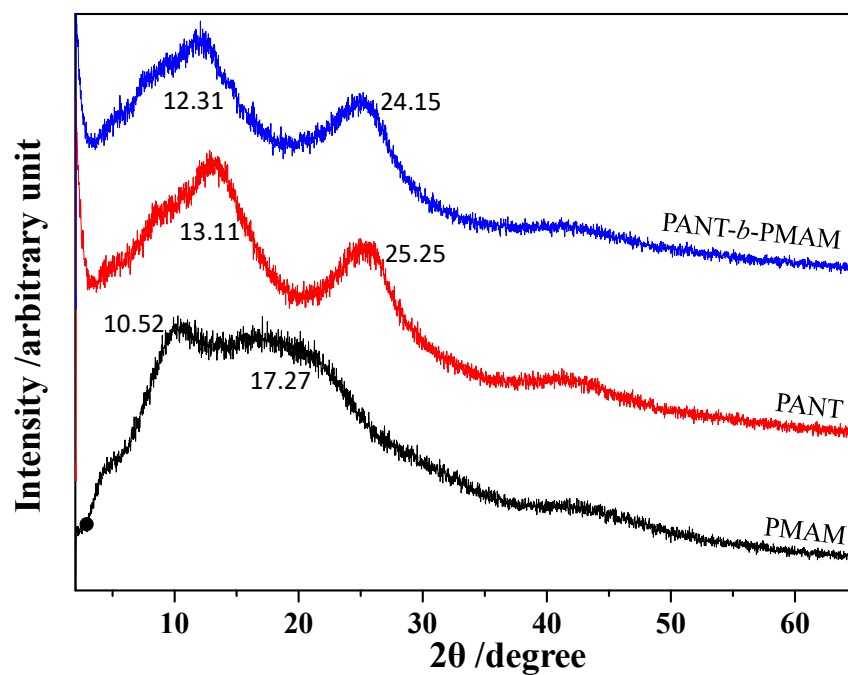


Figure A15. Powder X-ray diffraction curves of the synthesized polymers. X-ray diffractograms: CuK α radiation (land continuous) ($\lambda=1.54 \text{ \AA}$) at a scan speed of $0.045^\circ \text{ min}^{-1}$.

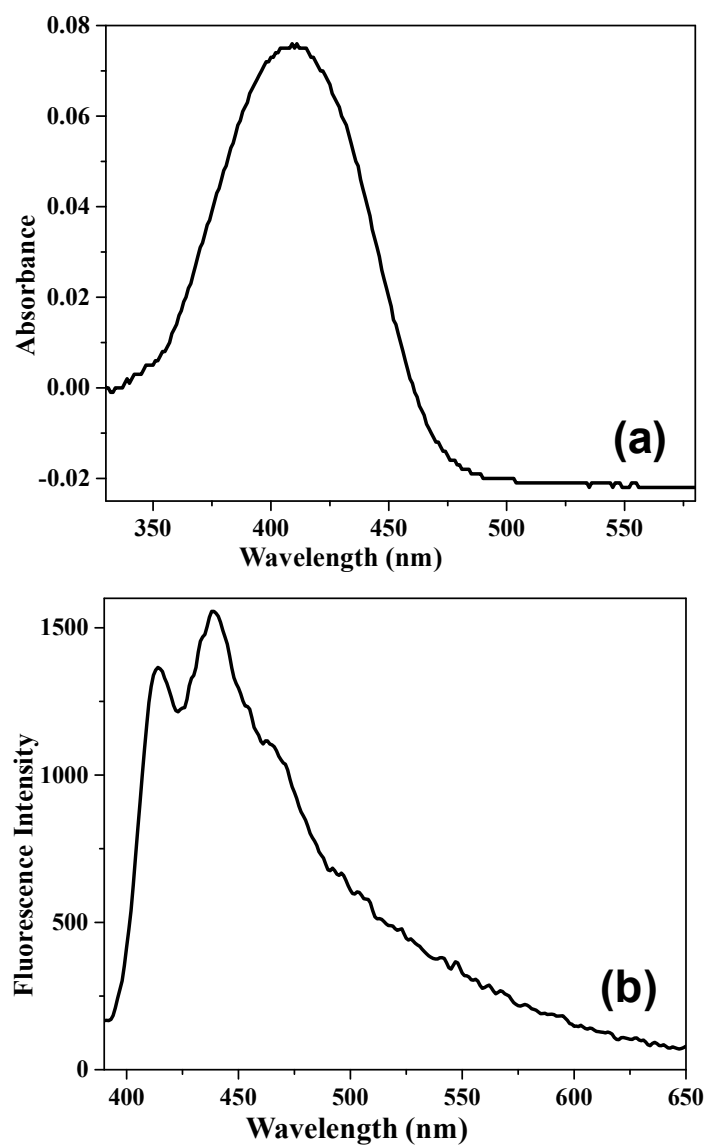


Figure A16. (a) UV-vis and (b) fluorescence spectra of the ANT monomer in DMSO solution.

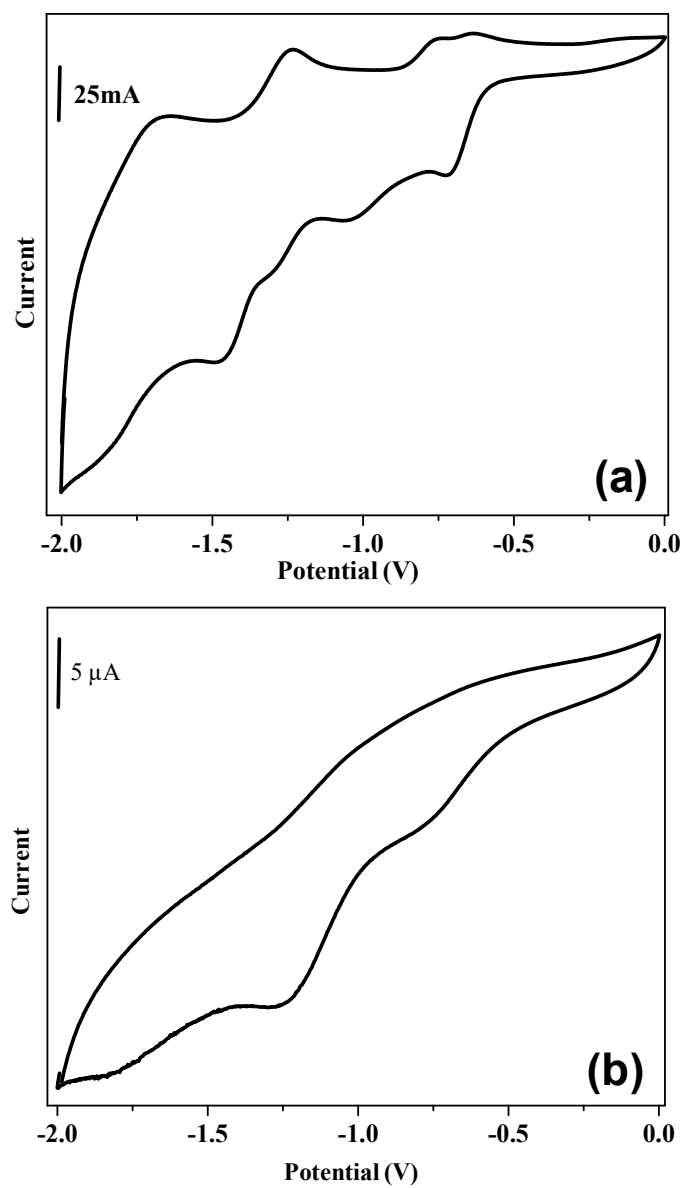


Figure A17. Cyclic voltammetry curves of (a) ANT and (b) MAM monomers in DMF (10 mM).

Table A1. Synthesized polymers yields and molecular weights.

Polymer code	Yield (%)	¹ H-NMR spectrum	Molecular weight ^a by SEC	
			M _w (g/mol)	Đ
PANT	71	4434 ^a	3562	1.1
PANT- <i>b</i> -PMAM	70	9540 ^b	11319	1.4
PMAM	68	8148 ^c	7811	1.20

^a $ANT_{fw} \times (I_{0.8} \text{ compared to } I_{6.7-9.2}) + T_{fw}$; where, ANT_{fw} : ANT molecular weight; $I_{6.7-9.2}$: intensities in ¹H-NMR spectra at δ 6.7-9.2 pendent anthraquinone aromatic ring proton; $I_{0.8}$: at δ 0.8 ppm RAFT agent methyl protons and T_{fw} : RAFT agent fragments molecular weight (280) at PANT chain terminal ends.

^b $[ANT_{fw} + MAM_{fw}] \times (I_{0.84} \text{ compared to } I_{8-9} \text{ and } I_{6.2}) + T_{fw}$; where, ANT_{fw} : ANT molecular weight; MAM_{fw} : MAM molecular weight; I_{8-9} : intensities in ¹H-NMR spectrum at δ 8-9 ppm pendent anthraquinone aromatic ring proton; $I_{6.2}$: maltose anomeric proton δ 6.2 ppm; $I_{0.84}$: δ 0.84 ppm RAFT agent methyl protons and T_{fw} : RAFT agent fragments molecular weight (280) at PANT-*b*-PMAM chain terminal ends.

^c $MAM_{fw} \times (I_{1.9-2.2} \text{ compared to } I_{1.4}) + T_{fw}$; where, MAM_{fw} : MAM molecular weight, $I_{1.9-2.2}$: intensities in ¹H-NMR spectra at δ 1.9-2.2 ppm methacrylated methyl proton; $I_{1.4}$: at δ 1.4 ppm terminal methyl protons and T_{fw} : ATRP initiator fragments molecular weight (195) at PMAM chain terminal ends.

Table A2. Thermal characteristics of the synthesized polymers.

Polymer code	TGA ^a (°C)			DSC ^b (°C)		
				% Char	T _m ^c	
	T _{d5%}	T _{d10%}	T _{onset}	at 750 °C	T _g	(ΔH J/g)
PANT	300	333	367	26.6	36	166 (0.30)
PANT- <i>b</i> -PMAM	297	320	354	27.6	39	170 (0.97)
PMAM	284	294	288	10.4	48	159 (0.95)

^aunder N₂ atmosphere; ^bdata on second heating; ^cpeak temperature.

Table A3. Photochemical properties of the PANT and PANT-*b*-PMAM.

Polymer code	λ _{max} ^a (nm)	Emission						
		λ _{max} ^b (nm)	Δλ _{max} ^c	E _{onset} ^{red} ^d (V)	E _{LUMO} ^e (eV)	λ _{onset} ^f	E _g ^g (eV)	E _{HOMO} ^h (eV)
PANT	410.1	435.70	25.6	-0.1752	-4.6248	500.13	2.47	-7.0948
PANT- <i>b</i> -PMAM	412.1	437.66	25.56	-0.2954	-4.5046	497.42	2.49	-6.9966

^afrom UV-vis spectrum in DMSO; ^bfrom fluorescence spectrum in DMSO, ^cemission λ_{max}-λ_{max},

^dCV curve onset value, ^e=(4.80 + E_{onset}^{red}), ^fUV-vis spectrum onset value, ^gCalculated from

E_g=1240/λ_{onset}(UV-Vis), ^h=E_{LUMO}-E_g.